catalysts

MDPI

Review

Two-Dimensional Nanostructures in the World of Advanced Oxidation Processes

Dominika Ścieżyńska [1], Dominika Bury [2], Piotr Marcinowski [2], Jan Bogacki [1,*], Michał Jakubczak [1] and Agnieszka Jastrzębska [2]

[1] Faculty of Building Services, Hydro and Environmental Engineering, Warsaw University of Technology, Nowowiejska 20, 00-653 Warsaw, Poland; dominika.sciezynska.dokt@pw.edu.pl (D.Ś.); michal.jakubczak.dokt@pw.edu.pl (M.J.)

[2] Faculty of Materials Science and Engineering, Warsaw University of Technology, Wołoska 141, 02-507 Warsaw, Poland; dominika.bury.dokt@pw.edu.pl (D.B.); piotr.marcinowski@pw.edu.pl (P.M.); agnieszka.jastrzebska@pw.edu.pl (A.J.)

* Correspondence: jan.bogacki@pw.edu.pl

Abstract: Two-dimensional compounds with nanostructural features are attracting attention from researchers worldwide. Their multitude of applications in various fields and vast potential for future technology advancements are successively increasing the research progress. Wastewater treatment and preventing dangerous substances from entering the environment have become important aspects due to the increasing environmental awareness, and increasing consumer demands have resulted in the appearance of new, often nonbiodegradable compounds. In this review, we focus on using the most promising 2D materials, such as MXenes, Bi_2WO_6, and MOFs, as catalysts in the modification of the Fenton process to degrade nonbiodegradable compounds. We analyze the efficiency of the process, its toxicity, previous environmental applications, and the stability and reusability of the catalyst. We also discuss the catalyst's mechanisms of action. Collectively, this work provides insight into the possibility of implementing 2D material-based catalysts for industrial and urban wastewater treatment.

Keywords: 2D structures; MXenes; Bi_2WO_6; MOFs; Fenton process; wastewater treatment

check for updates

Citation: Ścieżyńska, D.; Bury, D.; Marcinowski, P.; Bogacki, J.; Jakubczak, M.; Jastrzębska, A. Two-Dimensional Nanostructures in the World of Advanced Oxidation Processes. *Catalysts* **2022**, *12*, 358. https://doi.org/10.3390/catal12040358

Academic Editor: Monica Baia

Received: 29 December 2021
Accepted: 18 March 2022
Published: 23 March 2022

Publisher's Note: MDPI stays neutral with regard to jurisdictional claims in published maps and institutional affiliations.

Copyright: © 2022 by the authors. Licensee MDPI, Basel, Switzerland. This article is an open access article distributed under the terms and conditions of the Creative Commons Attribution (CC BY) license (https://creativecommons.org/licenses/by/4.0/).

1. Introduction

Many industrial productions, especially chemical, pharmaceutical, and cosmetic, are associated with generating a large amount of postproduction wastewater. These kinds of industrial wastewaters mainly come from washing process lines with disinfectants and surfactants [1–3]. The quantitative and qualitative composition of sewage is closely related to the production profile of the plant and the cleaning solutions [1,4]. The multitude and complexity of compounds in industrial wastewater represent a significant threat to the proper functioning of wastewater treatment plants and the environment [5]. The obligations of the supplier of industrial wastewater discharged to sewerage facilities include compliance with the requirements concerning the quality of wastewater pollutant parameters. Unfortunately, the concentration limits of wastewater discharged into the sewerage system or treatment plant are often exceeded. Even a small portion of wastewater (containing an undesirable or too high concentration of substances) introduced into a biological reactor may cause rapid and negative changes to its biocenosis and performance [6]. Therefore, it is necessary to carry out a preliminary wastewater purification before it is transferred to the treatment plant (Figure 1) [3–5,7].

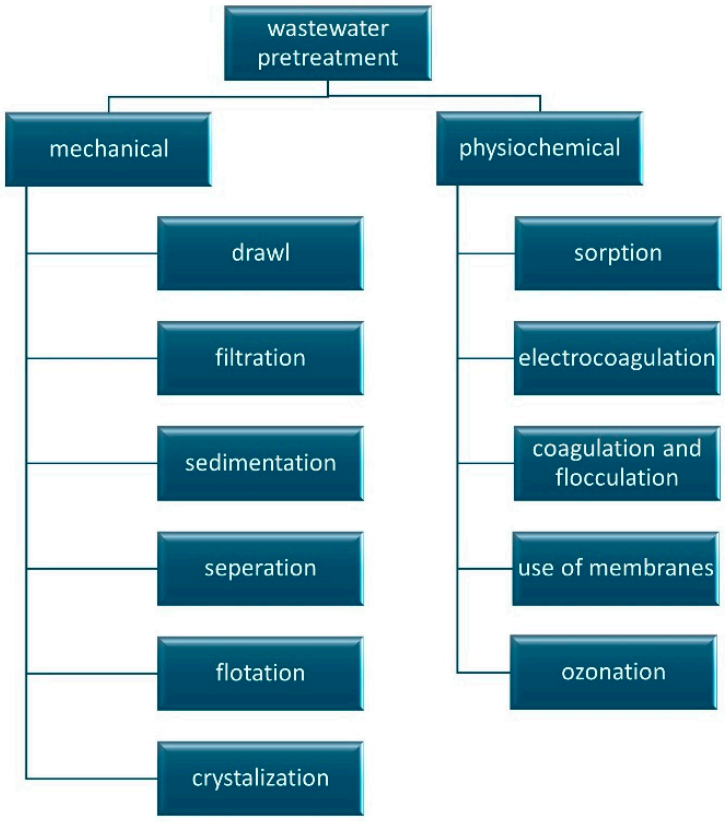

Figure 1. Preliminary wastewater treatment methods.

Mechanical wastewater treatments, such as filtration, drainage, sedimentation, and flotation processes, are intended to eliminate larger floating and dragged solids, granular particles, easily falling suspensions, oils, and fats [8]. The treatment efficiency relies heavily upon the chemical properties of contaminants and operating conditions. Therefore, it is common to combine different treatment processes for a more efficient wastewater treatment. The most attractive and favorable option for the effective removal of organic pollutants in wastewater is represented by advanced oxidation processes (AOPs) [9]. They can be used alone or as one of the purification steps [10]. Since the concept of AOPs was proposed in the 1980s for drinking water treatment, they have been broadly applied for the treatment of different types of wastewater [11–19].

The mechanism of AOPs is based on the oxidation of organic compounds to carbon dioxide, water, and inorganic ions, or at least to harmless products, using hydroxyl radicals ($^{\bullet}$OH) and other radicals with a high redox potential (Table 1) [20]. To initiate oxidation for wastewater treatment, most AOPs are based on the generation of hydroxyl radicals due to their highly oxidizing properties [20,21]. Hydroxyl radicals owe their potential to the presence of an unpaired electron in the structure and a half-life of less than 10^{-9} s [22]. The formation of hydroxyl radicals can be achieved via chemical, sonochemical, photochemical, and electrochemical processes and their combination using various oxidants (H_2O_2 and O_3). Other AOPs include ionizing radiation, nonthermal plasma, and supercritical water oxidation. A schematic classification of advanced oxidation processes is presented in Figure 2 [23].

Table 1. A comparison of the oxidative potential of various oxidizing agents.

Oxidizing Agent	Potential (V)
Fluorine (F_2)	3.03
Hydroxyl radical ($HO^{\bullet}$)	2.80
Atomic oxygen (O)	2.42
Ozone (O_3)	2.07
Hydrogen peroxide (H_2O_2)	1.78
Perhydroxyl radical ($^{\bullet}OOH$)	1.70
Permanganate ($KMnO_4$)	1.68
Chlorine (Cl_2)	1.36
Molecular oxygen (O_2)	1.23

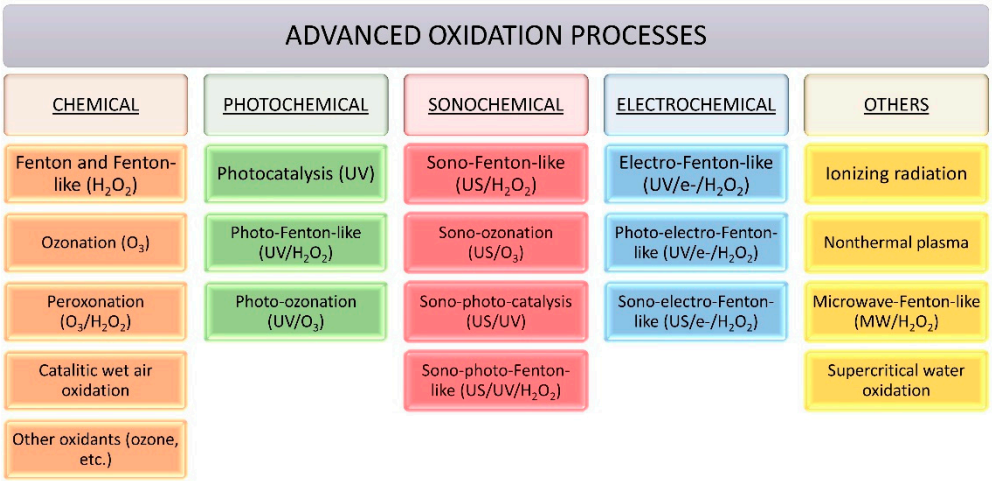

Figure 2. Classification of advanced oxidation processes.

The Fenton process is an AOP [24]. The classical Fenton process uses the reaction of hydrogen peroxide (H_2O_2) with an iron (II) ion, which is based on the production of hydroxyl radicals [23]. The prominent advantage of this technology is its simplicity, good repeatability, and easy handling [24]. The efficiency of the classical Fenton process is influenced by many factors, i.e., the pH, type of substances present in the wastewater, dose and ratio of reactants, reaction time, and temperature [16–19,25–29]. The pH of the solution determines the correct course of the process. To be effective, the Fenton process requires an acidic environment (pH 3–5) [16,17,28]. The optimum temperature range for the process is 10–40 °C [24]. Above this range, the decomposition of hydrogen peroxide into water and oxygen is accelerated. Consequently, hydrogen peroxide is not fully utilized efficiently for the production of hydroxyl radicals [30–32].

The amount of peroxide required for the process depends on the contaminants present in the wastewater and their presumed degree of degradation [31]. The main disadvantage of applying the classical homogeneous Fenton process is the generation of secondary sludge produced in the neutralization step of the treated wastewater [16,32]. Ferric and ferrous ions in the treated wastewater produce hydroxide precipitates, which must be removed after the process. Moreover, the system must be operated under a stringent pH control due to the oxidation activity of $^{\bullet}OH$ and the long-term instability of the catalysts. Furthermore, $^{\bullet}OH$ radicals are not continuously generated, which limits the reaction time. All these factors add cost and complexity to the process [33]. Due to process disadvantages, it is no surprise that considerable effort has been devoted to looking for alternative ways to conduct such a heterogeneous Fenton process.

A heterogeneous system can optimize the conventional Fenton process by replacing a homogeneous solution of iron ions with a solid catalyst containing active catalytic components. As a result, there is a decrease in the production of iron sludge due to the low level of iron ions leaching from catalysts [34]. Although many improvements are provided by

a heterogeneous system, issues relate to the long-term instability of the catalysts. Moreover, high amounts of H_2O_2 are required to provide efficient levels of $^{\bullet}OH$, and this can be difficult as there are many competitive reactions in the Fenton reaction system [33].

One of the most popular forms of the heterogeneous Fenton process modification is based on ultraviolet (UV) light irradiation [35]. This is called photocatalytic modification (or simply, the photo-Fenton process) and is induced by photons accelerating the catalytic reaction. Ultraviolet radiation can be successfully used in both heterogeneous and homogeneous reactions [16,17,36–38]. The photo-Fenton process with slow reaction kinetics is characterized by a low yield of available charge carriers and active radicals; thus, researchers have aimed at modifying the process to obtain a higher effectiveness [38].

Electrochemical modification introduced to the Fenton process is intended to allow the Fenton reagent to be produced continuously and in a controlled manner in an electrochemical reactor. In the electrochemical process, a two-electron reduction in an oxygen molecule (O_2) from compressed air occurs, resulting in the in situ generation of H_2O_2. It is also possible to dissolve the iron electrode to produce Fe^{2+} ions [39].

The use of the aforementioned heterocatalyst in the Fenton process improves the process by introducing additional mechanisms to promote wastewater treatment. Nevertheless, heterogeneous processes are not fully understood. Scientists are still looking to optimize the process by increasing its efficiency, reducing running costs (e.g., by reusing the catalyst), and eliminating process defects (e.g., eliminating large amounts of sludge generated after the process). They have experimented with different modifications of the Fenton process and studied the properties of various materials to identify those with the greatest benefit. The discovery of graphene and its many properties has drawn scientists' attention to the possibility of using 2D materials in the modified Fenton process. They began looking for materials whose properties would allow the process to be carried out as efficiently as possible, including a reduction in the number of reactants used and an increase in the surface-to-volume ratio to minimize the amount of sludge produced after the process.

This review deals with the use of modifications applied to the Fenton process using two-dimensional compounds, including two-dimensional transition metal carbides, nitrides, or carbonitrides (i.e., MXenes) for the treatment of wastewater containing different kinds of micropollutants dissolved in wastewater, i.e., bezafibrate, bisphenol A, fluoxetine, naproxen, antibiotics, herbicides, and other dangerous substances depending on the specifics of the plant.

2. Two-Dimensional Nanostructures

Various two-dimensional (2D) nanomaterials are characterized by their unique shape, such as sheet-like structures with atomic to nanoscale thicknesses [40–42]. Two-dimensional nanostructures are characterized by a high specific surface area and outstanding physicochemical properties. Two-dimensional materials are characterized by a large surface-to-volume ratio and adsorption potential, which additionally support processes [43–45]. Therefore, they can be used in many applications and processes [42–48], including AOPs [43–45]. Two-dimensional materials have been popularized since the discovery of graphene, which reflects the previously mentioned properties. However, graphene cannot be used in many processes because of its many disadvantages, such as its gapless band structure and low chemical reactivity [46–50]. Therefore, scientists started using other elements to prepare new 2D nanostructures. The increased popularity of 2D compounds has accelerated the synthesis of new compounds. Bi_2WO_6 (BWO), MOF, and MXenes are the most popular 2D nanostructures used in the Fenton process [43].

Due to their distinctive structures and novel properties, these nanostructures have attracted increasing attention as an option for an efficient environmental remediation, including wastewater treatment. The development of various 2D compounds can optimize their properties and produce effective results in the process. However, only a few 2D materials in this area have been studied to date, which determines the need for a more thorough exploration of this topic.

3. MXenes

MXenes are new, innovative 2D transition metal carbides, nitrides, and carbonitrides discovered in 2011 by researchers from Drexel University [51]. These new interesting 2D materials are prepared from multilayered carbides called "MAX" phases (M is a transition metal, A refers to elements from groups 13 and 14 on the periodic table, and X is carbon and/or nitrogen) [52]. The synthesis of MXenes is often based on etching atomically thin layers of A in MAX phases followed by a further delamination. The formula of MXenes is $M_{n+1}X_nT_x$, where M is an early transition metal (such as Sc, Ti, Zr, Hf, V, Nb, Ta, Cr, Mo, or Mn), X is C and/or N (n = 1, 2, or 3), T refers to a surface termination unit (e.g., hydroxyl, oxygen, or fluorine), and x represents the number of surface functionalities [45,53–55]. Currently, scientists have obtained over 70 types of different MAX phases and about 30 kinds of MXenes. According to theoretical calculations, it is possible to discover even more interesting MXenes with unique properties. MXenes have highly variable characteristics, a great level of stoichiometry, and a number of surface functions. Moreover, scientists can adjust the physical and chemical properties of these compounds to their specific applications. Therefore, they have grabbed the interest of researchers from all over the world [49,50,56]. One of the most popular MXenes is Ti_3C_2 due to its additional advantages, such as the presence of titanium oxide on its surface, which serves as a lattice shuttle for electron transfer in H_2O_2 activation [49,57–59]. Therefore, scientists have implemented Ti_3C_2 in many applications, as shown in Figure 3.

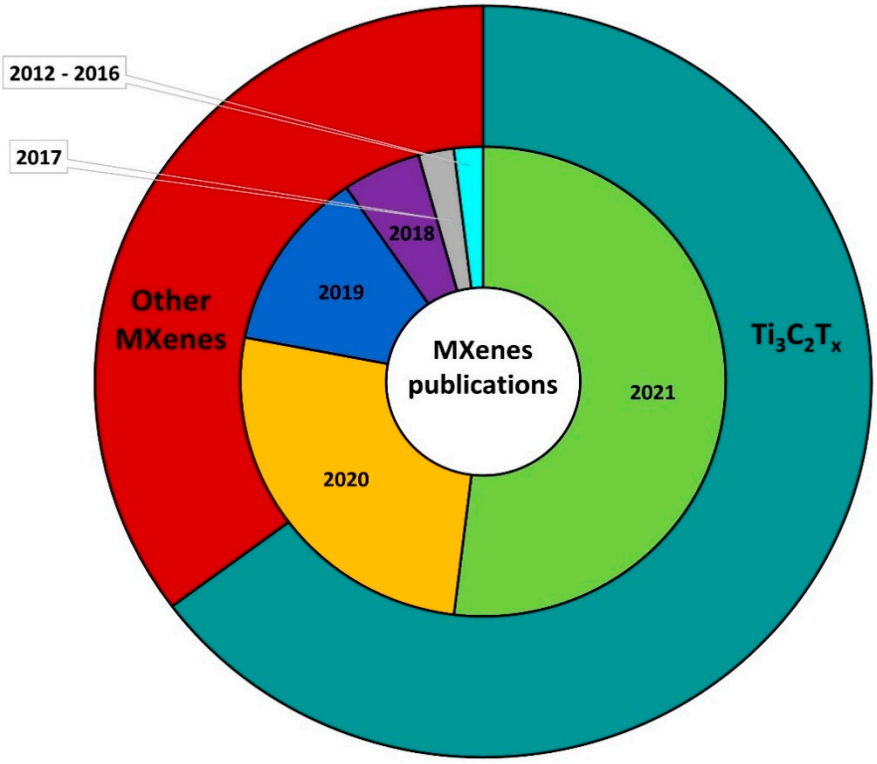

Figure 3. Number of publications concerning MXenes up to the year 2021, showing the growing interest in MXenes according to the ScienceDirect database. The external ring illustrates the number of publications related to the $Ti_3C_2T_x$ MXene in comparison to other MXenes up to the year 2021, while the inner ring shows the number of publications concerning MXenes per year.

MXenes are used in assisted energy storage and conversion [60], catalysis [61], sensors [62], electronics [63], and biomedical applications [49,50,64,65] due to their interesting properties. Recent results have also shown that MXenes can be utilized in environmental adsorption. Moreover, they are promising adsorbents for the removal of environmental pollutants from aqueous solutions [66,67]. One of the most important aspects of the efficiency

process is the even dispersion of catalyst particles on the hydrophilic and conductive MXene matrix surfaces [64]. This is crucial due to the fast charge transfer and target pollutant adsorption during AOPs, especially the Fenton process. Moreover, MXenes can immobilize Fenton reagents inside the layer spaces due to their unique 2D layered nanostructure and sheet surface electronegativity. Moreover, they can improve the distribution of functional nanoparticles. Recent results showed that MXenes are a great alternative to iron-based heterogeneous Fenton reagents [68].

MXenes have a high negative zeta potential, enabling the formation of a stable colloidal solution in water [56,69,70]. Their functionalized surface guarantees the hydrophilic nature of MXenes and the possibility to bond to various compounds. Moreover, these 2D structures with a fast charge transfer are characterized by a large surface area. Additionally, scientists have noted that the bandgap of MXenes is tunable. These properties are very important when using MXenes in AOPs. Interestingly, scientists have obtained the high-level accessibility and modification of the active sites. Furthermore, MXene elements are flexible and adjustable [67]. Results of various analyses showed that they have potential applications such as ion intercalation (Na^+, K^+, NH_4^+, etc.) and catalyst immobilization (metal, metal oxides, etc.) [71]. These unique 2D structures can also be recycled. Moreover, the process is aided by the ability to cycle between low- and high-valence states.

Cheng et al. [72] prepared MXenes with titanium dioxide (TiO_2) nanoparticles via the hydrothermal method. These 2D structures were identified as a good source of active low-valence titanium species. They were called "microporous MXene–TiO_{2-x} nanodots". These catalysts were characterized by a porous structure, fulfilled by monolayered MXene nanoflakes, which acted as the skeleton. Moreover, TiO_{2-x} nanodots were embedded evenly on the MXene flakes. The authors obtained a high catalytic efficiency in organic pollutant degradation (96% degradation of rhodamine B (RhB) in 10 min), with a low catalyst concentration (0.25 g/L) and amount of H_2O_2 (0.7 mM). These advantages distinguish the Fenton process using MXenes as catalysts in wastewater removal [72].

Cui et al. [67] prepared composites of titanium carbide (Ti_3C_2) MXene and magnetite (Fe_3O_4) magnetic nanoparticles to degrade methylene blue, often used as a dye and medication, in a concentration of 20 mg/L. The authors utilized dopamine to obtain polydopamine to coat the catalyst surface and coordinate the process generation of Fe_3O_4 magnetic nanoparticles on the MXene surface. The advantage of this process was its minimal catalyst concentration (0.2 g/L) needed to remove pollutants (97.09% removal). Additionally, Cui et al. [67] conducted the Fenton process using MXenes as the catalyst to degrade methylene blue in relatively mild reaction conditions (pH = 3; time = 1 min; temperature = 30 °C). Moreover, they obtained a high degradation efficiency in cyclic operation (71.5% degradation after five cycles compared to 96% after the first cycle). This innovative method of pollutant degradation was also characterized by a simple operation process. In addition, only small changes in efficiency were observed over a wide range of pH, decreasing below 80% at a pH of 9 and higher. These results suggest that MXenes could be reliable in the practical application of organic pollutant removal [67].

Ma et al. [68] prepared new innovative magnetic nanoscale zero-valent iron-based MXene nanosheets (nZVI)@Ti_3C_2. The results showed a synergistic effect of both compounds on enhancing the chemical reactivity and stability of the catalyst. Interestingly, additive MXenes to the nZVI restrained the agglomeration of nZVI particles. Moreover, the authors noted an improved promotion of electron transfer between magnetic particles approximately 10–40 nm in diameter in these composites. Interestingly, processes with nZVI@Ti_3C_2 as catalysts were efficient across a wide pH range (92.7%, 91.1%, 87.6%, 81.3%, 72.2%, and 37.2% removal at a pH of 3, 4.5, 6, 7, 8, and 9, respectively). This effect was not observed in homogeneous Fenton oxidation. Moreover, the catalytic activation acted mainly via surface sites in the classical Fenton process. Additionally, Ma et al. [68] noticed the dissolution of ferrous ions, which enabled effective pollutant degradation [68].

Due to their high conductivity and specific surface, MXenes have demonstrated wide applications in many fields. The multiple confirmations of their stability and flexibility

in terms of synthesis with other compounds have made MXenes a hot topic in the world. Their properties allow the assumption that MXenes may revolutionize current processes of wastewater treatment and the removal of undesirable substances. The ability to configure a compound with specific desired properties in tandem with their nanostructure could presumably reduce the problematic aspects of existing heterocatalytic processes. However, the use of these compounds is in its infancy; hence, it is necessary to study them more closely to understand the mechanisms underlying specific processes, including degradation.

4. Bi_2WO_6 (BWO)

Bismuth tungstate (Bi_2WO_6, BWO) is a popular ternary metal oxide, which is also used as a catalyst in AOPs, including the Fenton process and its modifications. This interesting 2D structure is an n-type semiconductor belonging to the perovskite family. Bi_2WO_6 is described by the formula $Bi_2A_{n-1}B_nO_{3n+3}$, in which A represents a large cation with 12 coordinates (such as Ca, Pb, Sr, Bi, or Ba), while B is a smaller cation with 6 coordinates (Ti, Fe, Mo, Ta, or W), and n = 1. This compound is one of the intermediate oxides with related crystal structures found in the Bi_2O_3–WO_3 pseudo-binary phase system. However, Bi_2WO_6 has a higher visible-light photocatalytic activity than Bi_2O_3 and WO_3 [70,73].

One of the essential problems with using catalysts in AOPs is the rapid recombination of charge carriers [74]. However, this disadvantage is eliminated by the modification of the compound. Other disadvantages are the high recombination and quickly photogenerated electron–hole pairs [75]. The appropriate modification of BWO causes the production of a heterojunction, which is an effective method for separating photogenerated carriers and widening the light-responsive region [73].

Bismuth tungstate is an excellent photocatalyst with the unique absorbance of photons in the visible-light region. This interesting 2D structure has a lower energy gap than the popular TiO_2 photocatalyst (2.8 eV vs. 3.10 eV for TiO_2) [76,77]. Moreover, Bi_2WO_6 has favorable chemical and physical properties. Additionally, bismuth tungstate is characterized by nontoxicity, photostability, favorable electronic and catalytic behavior, ferroelectric piezoelectricity, and nonlinear dielectric susceptibility [60]. BWO has a high-valence band potential and many active sites, which are important for the efficient process of pollutant degradation [78]. Due to its unique photocatalytic properties, BWO is readily used in the photo-Fenton process [70].

Guo et al. [79] modified BWO by adding Cu_2ZnSnS_4, which could respond to visible and near-infrared light and combine with other semiconductors as an effective cocatalyst. As a result, the authors obtained a semiconductor with a narrow energy gap, which could increase photocatalytic activity. They synthesized Cu_2ZnSnS_4/Bi_2WO_6 (CZTS/BWO) to reinforce the photocatalytic properties of the catalysts. Although BWO has a 2D structure and CZTS has a 3D spherical structure, TEM images confirmed that, together, they formed a 2D/2D structure. Excellent results were obtained (from a 20% and 62% removal of rhodamine blue using CZTS and BWO alone, respectively, to a 94% removal using complex CZTS/BWO as a catalyst) due to the increase in active sites of BWO (with the surface composition and elemental valence increasing the possibility of reaction), which expanded the solar spectral response range and accelerated the cycle of Cu(II)/Cu(I) [79].

Jiang et al. [80] matched the band structures of BWO and $CuFe_2O_4$ (CFO). Results showed that BWO could be a prime material for constructing an intimate p–n heterojunction to remove pollutants. The authors prepared a magnetic p–n $Bi_2WO_6/CoFe_2O_4$, which was used as a catalyst to remove tetracycline hydrochloride in AOPs. BWO was synthesized via an easy hydrothermal method with bismuth nitrate dissolved into solution, including acetic acid and water. In the next step, scientists added disodium hydrogen phosphate as a buffer to obtain a stable solution. After mixing and heating the solution, BWO was prepared. The results revealed strong optical properties in the wavelength range of 300–800 nm. Interestingly, the visible-light absorption decreased with the increased amount of loading of BWO. This could be the effect of the weak visible-light absorption of pristine BWO in contrast to intrinsic wide bandgaps such as 1.90 eV for CFO and 2.85 eV for BWO [80].

In another interesting study, Zhong et al. [81] prepared a series of Cu(II)-doped Bi_2WO_6 nanomaterials with good photo-response properties. They were utilized to optimize the activity of peroxymonosulfate (PMS) in removing norfloxacin (NOF). They noted an efficient NOF degradation after 60 min in a wide pH range from 3.3 to 10.7 [81].

It seems that BWOs have a high potential and can be successfully used in wastewater treatment. However, the main drawbacks of BWOs are the boundedness of the visible-light response region and the high recombination rate of the photogenerated electron–hole pairs in the photocatalysis process. A way to eliminate these problems is to create BWO complexes with other compounds, thereby adapting and modifying the properties of the compound according to the needs.

5. MOF

Metal–organic frameworks (MOFs) are crystalline materials newly applied to AOPs and modifications of the Fenton process. These interesting compounds are composed of inorganic nodes or vertices in a framework consisting of metal ions [82]. Examples of vertices in the framework could be Cr(III), Fe(III), Al(III), Mn(II), or clusters (i.e., secondary building units (SBUs)) such as $Zn_4O(COO)_6$ or $Cu_2(COO)_4$. Moreover, the components of the nodes of MOFs are characterized as carboxylates, which are connected by coordination bonds to organic linkers [83]. Additionally, SBUs encompass structural nodes and present as metal ions plus nonmetals. Therefore, MOFs are characterized by an elementary diversity in terms of topology, connectivity, and function. Interestingly, new, innovative SBUs include most transition metals and several main-group metals. Other forms are alkali metals, alkaline earth metals, lanthanides, and actinides [84]. These interesting materials also have a large surface area (1000 to 10,000 $m^2 \cdot g^{-1}$), high porosity, and flexible tolerability. Diversified structures characterize MOFs with highly tunable pore sizes (usually 0–3 nm, up to 9.8 nm) [85]. Moreover, scientists have noted that these compounds have many metal nodes and a theoretically unlimited number of organic linkers. Therefore, the compositions and structures of MOFs can be easily tuned [86].

An interesting form of MOFs is represented by two-dimensional (2D) nanosheets. MOF nanosheets have more active metal sites available toward the reactants and stronger electron transfer than other forms of MOFs. Moreover, active sites are more open and accessible. Additionally, scientists have noted a uniform dispersion of active sites throughout MOFs. Interestingly, the enrichment of substrate molecules around the active sites causes additional activation and catalytic conversion. The diffusion barrier for molecules becomes smaller during the process, making them more efficient. These properties promote the adsorption and decomposition of H_2O_2 molecules [87,88].

Additionally, the 2D morphologies of MOFs vary significantly with a high lateral-to-thickness aspect ratio. Moreover, it is facile to access active sites due to the highly ordered pores. Scientists have also noted the transport of substrates and products to MOF pores, which can be tuned from microporous to macroporous. Therefore, scientists can control pore size and shape. This effect is necessary for the accessibility of reaction substrates with specific parameters. Thus, it is possible to differentiate similar substrates, which favors the potential application of MOFs to catalysis, especially in AOPs [89].

Additionally, unsaturated metal sites and functional groups on the MOF surface amplify its catalytic properties. Scientists have coordinated metal ions with ligands and solvent molecules, which are readily removed by heating or vacuum. Moreover, they retained the MOF structures during this process and created unsaturated metal sites (CUS). The CUS accepts electrons from the substrates and promotes their conversion to products. Additionally, a benefit to an effective catalysis is the presence of functional groups on organic linkers on MOF structures [90,91]. The presence of various functional groups increases the number of active sites for catalysis [92,93]. Interestingly, scientists have noted that functional groups with catalytically active properties can be added to the organic linkers of MOF structures [94,95].

Scientists have modified MOFs to obtain improved catalytical properties. Fe-MOFs are popular catalysts in Fenton-based AOPs due to the Fe(III)/Fe(II) interconversion and the presence of photosensitive Fe−O clusters [96]. Additionally, the Fe included in MOF structures is nontoxic, easily accessible, and commonly present in minerals from the Earth's crust. Moreover, FeMOFs have intensive absorption in the visible-light region due to the existence of numerous iron–oxo (Fe–O) clusters. Fe-MOFs are popular catalysts in photocatalytic pollutant degradation, carbon dioxide reduction, oxygen evolution, and AOPs, especially the Fenton process. The essential mechanisms of this process are related to the photoexcitation of Fe–O clusters and the electron transfer from O(II) to Fe(III) [97]. In other research, scientists prepared Co-MOFs with coordinated water in their structure, providing more open access to reactants. Due to the high oxidation states of nickel species, scientists obtained remarkable activity and favorable kinetics of the ultrathin Ni-MOF electrocatalysts [83]. Mixing this catalyst with black acetylene resulted in excellent HER catalytic activity with a low onset potential of 18 mV and long-term stability [98,99].

In the photo-Fenton process, one study applied a series of Fe-based MOFs for organic pollutant removal [88]. Soetaredjo et al. [100] prepared a flexible Fe-MOF (MIL-88B) under mild subcritical water (SCW) conditions (100 °C). This unique structure had a micro-bipyramidal form. Accordingly, these compounds were characterized by large pore channels (∼32 nm) and open iron sites. The authors showed a higher mineralization efficiency compared to traditional homogeneous Fenton ($FeSO_4/H_2O_2$) and Fenton-SCW processes [100].

Wu et al. [88] prepared typical Fe-MOFs with organic ligands, such as benzene-1,4-dicarboxylate, which were used as a catalyst in the Fenton-like process to degrade tetracycline hydrochloride (TCH). Moreover, they used visible light to accelerate the Fe(II)/Fe(III) cycle. Results showed that the process with MOFs was more efficient compared to conventional Fenton-like catalysts such as Fe_2O_3. The excellent results were related to the large surface area, pore volume, and coordinatively unsaturated iron sites. Additionally, the authors obtained a synergistic effect between photocatalysis and the Fenton-like process visible-light system. This was the effect of the efficient separation and migration of photo-generated carriers. Moreover, the authors noted that the optimal range of pH was further broadened to 10.2. Interestingly, simulative solar light was more efficient than visible light [88].

Ye et al. [101] prepared Fe-MOFs with 2,2′-bipyridine-5,5′-dicarboxylate (bpydc) as the linker to degrade organic micropollutants via the photoelectro-Fenton treatment. The results showed a high removal efficiency of organic micropollutants such as bezafibrate at mild pH (pH range 3–7). Scientists obtained excellent results due to the numerous active sites, which enhanced the mass transport and charge transfer. During the process, Fe (II) was reduced to Fe (III) with photoinduced electrons (eCB^-) and UV/Vis photons. The applied catalyst behaved as an n-type semiconductor. These results confirmed that the photoinduced electrons were the major charge carriers [101].

Wang et al. [102] used a 2D micron-sized MOF sheet with Fe in the Fenton process to remove chloroquine phosphate. The catalyst was synthesized hydrothermally from $FeSO_4 \cdot 7H_2O$, 1,3-dibenzyl-2-imidazolidone-4,5-dicarboxylic acid (H_2L), and 4,4′-bipyridine. The process was carried out at pH 5 and organic pollutants were degraded efficiently (100%) after 30 min, presumably because of the structure of the catalyst complex, which allowed a fast mass transport and accessibility of the active sites.

Metal–organic frameworks are a new class of porous materials, characterized by a crystalline structure. Because of the tunability of their features, they are considered good candidates for wastewater treatment. Moreover, various applications have confirmed their versatility and high efficiency. Furthermore, their relatively low cost of production has encouraged scientists to further investigate these compounds. In potential wastewater treatment, the possibility of preparing materials with good adsorbent features and efficient photodegradation catalysis is the main incentive. However, there is still an urgent need to further investigate and implement MOFs in real conditions.

6. Mechanism of Modified Fenton Process with 2D Structures

Despite the rapidly increasing interest in the use of 2D structures for the destruction of harmful compounds and the treatment of industrial wastewater, the mechanisms of the process are not yet well understood.

The Fenton reaction is based on the generation of reactive oxygen species (ROS) capable of nonselectively oxidizing compounds in solution [103]. Hydroxyl radicals are most desirable because of their high reactivity potential. In order to carry out the classical Fenton process, it is necessary to provide reagents that react with the added H_2O_2 and generate those radicals. Currently, the best known and most effective process reagents are Fe^{2+} ions. There are also studies in which other ions (e.g., Cu^+) were successfully used in the Fenton process [80]. However, many reactions in the process also produce radicals with a lower potential (e.g., hydroperoxyl ($HO_2^{\bullet}$) radical or superoxide radical ($O_2^{\bullet -}$)) that can still successfully oxidize compounds (see Equations (9), (14) and (19)).

Depending on the composition of the wastewater and the substances it contains, the efficiency of the process may also be increased or decreased. For example, carbonate species (HCO_3^- and CO_3^-) are known hydroxyl radical scavengers. The reaction of hydroxyl radicals with carbonate compounds (HCO_3^- and CO_3^{2-}) results in carbonate radicals ($HCO_3^{\bullet}$ and $CO_3^{\bullet -}$) (see Equation (1)), which are transition species that can react with hydrogen peroxide to form the already mentioned hydroperoxyl or superoxide radicals (see Equation (2)). Process reactions may also be terminated by $CO_3^{\bullet -}$ reactions with $O_2^{\bullet -}$ at a pH above 8 due to the dominance of $CO_3^{\bullet -}$ under these conditions (see Equation (3)). The mechanistic reactions are as follows [104,105]:

$$^{\bullet}OH + HCO_3^-/CO_3^{2-} \rightarrow HCO_3^{\bullet}/CO_3^{\bullet -} + OH^- \quad (1)$$

$$HCO_3^{\bullet}/CO_3^{\bullet -} + H_2O_2/HO_2^- \rightarrow HO_2^{\bullet}/O_2^{\bullet -} + HCO_3^-/CO_3^{2-} \quad (2)$$

$$CO_3^{\bullet -} + O_2^{\bullet -} \rightarrow CO_3^{2-} + O_2 \quad (3)$$

To understand the mechanisms underlying the modification of the Fenton process using 2D materials, including MXenes, as a catalyst, scientists have experimented with, among other things, quenching ROS to study the dominant one in the process. Notably, most Fenton active systems involving 2D materials are based on composite systems. The proposed mechanisms of pollutant degradation can be described by the following equations [68]:

$$\text{Ranitidine} + Fe(s) \rightarrow \equiv\text{Fe-Ranitidine}. \quad (4)$$

$$\text{Ranitidine} + Fe_3O_4/\gamma\text{-}Fe_2O_{3(s)} \rightarrow \equiv Fe_3O_4/\gamma\text{-}Fe_2O_{3(s)}\text{-Ranitidine}. \quad (5)$$

$$Fe^0{}_{(s)} + 2H^+ \rightarrow \equiv Fe(II)/Fe(II) + \equiv Fe^0{\cdot}[H] \rightarrow H_{2(g)}\uparrow \quad (6)$$

$$Fe^{0(s)} + 2H_2O \rightarrow \equiv Fe(II)/Fe(II) + H_{2(g)}\uparrow + 2^{\bullet}OH. \quad (7)$$

$$\equiv Fe(II) + H_2O_2 + H^+ \rightarrow \equiv Fe(III) + {}^{\bullet}OH_{ads} + H_2O. \quad (8)$$

$$\equiv Fe(III) + H_2O_2 \rightarrow \equiv Fe(II) + HO_2^{\bullet} + H^+. \quad (9)$$

$$\equiv Fe(III) + HO_2^{\bullet} \rightarrow \equiv Fe(II) + O_2 + H^+. \quad (10)$$

$$Fe^0{}_{(s)} + 2 \equiv Fe(III) \leftrightarrow 3 \equiv Fe(II). \quad (11)$$

$$\equiv Fe^0{\cdot}[H] + 3 \equiv Fe(III) \leftrightarrow 4 \equiv Fe(II) + H^+. \quad (12)$$

$$Fe(II) + H_2O_2 + H^+ \rightarrow Fe(III) + {}^{\bullet}OH_{free} + H_2O. \quad (13)$$

$$Fe(III) + H_2O_2 \rightarrow Fe(II) + HO_2^{\bullet} + H^+. \quad (14)$$

$$Fe(III) + HO_2^{\bullet} \rightarrow Fe(II) + O_2 + H^+. \quad (15)$$

$$^{\bullet}OH_{ads}/{}^{\bullet}OH_{free} + \text{Ranitidine} \rightarrow \text{Degraded products}. \quad (16)$$

$$\equiv Fe^0{\cdot}[H] + \text{Ranitidine} \rightarrow \text{Degraded products}. \quad (17)$$

$$^{\bullet}OH + Fe(II) \rightarrow OH^{-} + Fe(III). \quad (18)$$

$$^{\bullet}OH + H_2O_2 \rightarrow H_2O + HO_2^{\bullet}. \quad (19)$$

$$HO_2^{\bullet} + HO_2^{\bullet} \rightarrow H_2O_2 + O_2. \quad (20)$$

$$^{\bullet}OH + HO_2^{\bullet} \rightarrow H_2O + O_2. \quad (21)$$

$$^{\bullet}OH + {}^{\bullet}OH \rightarrow H_2O_2. \quad (22)$$

The mechanism above was proposed by Ma et al. [68] while working on H_2O_2 activation and ranitidine degradation using magnetic nanoscale zero-valent iron (nZVI)@Ti_3C_2-based MXene nanosheets (nZVI@Ti_3C_2) with a H_2O_2 system under acidic conditions. The mechanism was divided into four groups: the adsorption of ranitidine on the catalyst surface (Equations (4) and (5)), generation of Fenton reagent in the nZVI@Ti_3C_2/H_2O_2 system (Equations (6) and (7)), generation of radicals capable of degrading ranitidine (Equations (8)–(17)), and possibly competitive reactions that may lead to a decrease in the efficiency of the process (Equations (18)–(22)). They noted that hydroxyl radicals have a dominant oxidative role in the process; hence, degradation depends on the number of hydroxyl radicals and catalyst active sites. After generating Fenton reagents in the nZVI@Ti_3C_2/H_2O_2 system, a heterogeneous process was initially observed, in which surface-bound hydroxyl radicals ($^{\bullet}OH_{ads}$) were generated. In an acidic environment, oxidative corrosion followed, leading to the catalyst's dissolution and leaching of Fe^{2+} and Fe^{3+}. This process, in turn, led to the initiation of homogeneous reactions. In conclusion, it was found that the catalytic decomposition depended mainly on bound and only later on free hydroxyl radicals. Adsorption on the surface of the solid catalyst in the equation is indicated by the symbol ≡. Simultaneously, competitive reactions emerged that interrupted the main degradation process [68].

Other groups of researchers (Cheng et al. [72] and Wu et al. [106]) proposed mechanisms underlying photo-Fenton processes. Both groups had similar conclusions regarding the radicals reacting in the process. For example, Cheng et al. [72] observed the mechanism of the photo-Fenton process using MXenes as a catalyst. They compared the process with UV light and in darkness. They noted the presence of low-valence titanium species (Ti(III)) near the surface of TiO_2, which initiated the pseudo-Fenton reaction in the dark. Therefore, $^{\bullet}OH$ radicals were generated to accelerate the oxidation of organic dye molecules. In the presence of light, photocatalysis was observed. During the process, photo-generated electrons (e^{-}) combined with dissolved oxygen molecules and generated $O_2^{\bullet-}$ radicals. Simultaneously, the photogenerated holes (h^{+}) were transferred to the hydroxyl-terminated Ti_3C_2 skeleton flakes. The researchers found that this was an effect of the difference in work function at the heterojunction interface [72]. Thus, the probable mechanism underlying the modified Fenton process using 2D materials as a catalyst in the presence of UV light is similar to the known mechanism of the Fenton modification using a heterogeneous catalyst (e.g., in the form of zero-valent iron flakes). It can be stated that, in the presence of UV radiation, the photolysis of the H_2O molecule and the photoreduction in Fe^{3+} ions to Fe^{2+} with the formation of hydroxyl radicals occur (see Equation (23)). The use of light can increase the efficiency of the process. At a wavelength of λ =300–580 nm, the reduction in Fe^{3+} ions ($Fe(OH)^{2+}$) to Fe^{2+} ions occurs, which further increases the pool of Fe^{2+} ions required for the process (see Equation (24)). At the wavelength of λ = 280 nm, the photolysis of water molecules takes place, as a result of which the number of hydroxyl radicals formed in the process increases (see Equation (25)).

$$Fe^{3+} + H_2O + h\nu \rightarrow Fe^{2+} + {}^{\bullet}OH + H^{+}. \quad (23)$$

$$Fe(OH)^{2+} + h\nu \rightarrow Fe^{2+} + {}^{\bullet}OH \text{ (wavelength } \lambda = 300\text{–}580 \text{ nm)} \quad (24)$$

$$H_2O_2 + h\nu \rightarrow 2{}^{\bullet}OH \text{ (wavelength } \lambda = 280 \text{ nm)}. \quad (25)$$

Research on reactive species to identify the dominant one participating in the process, as well as to propose a simple mechanism of the Fenton-like process, was also performed by Ye et al. [101] and Wang et al. [102]. The results allowed for the conclusion that hydroxyl radicals play the main role in the Fenton-like process, consistent with the findings of the authors mentioned above [101,102].

As already cited above, Ye et al. [101] used Fe-MOFs with 2,2′-bipyridine-5,5′-dicarboxylate (bpydc) as the linker to degrade organic micropollutants via a photoelectro-Fenton treatment. Equations (26)–(28) represent the reactions introduced in the process mechanism via electro modification. The generation of H_2O_2 occurs at the cathode (Equation (26)), while the production of Fe^{2+} occurs at the sacrificial anode (Equation (27)). In addition, the generation of hydroxyl radicals due to the oxidation of water molecules was also observed in the modified process (Equation (28)).

$$\text{Cathode: } O_2 + 2H^+ + 2e^- \rightarrow H_2O_2. \quad (26)$$

$$\text{Sacrificial anode: } Fe^0 \rightarrow Fe^{2+} + 2e^-. \quad (27)$$

$$H_2O \rightarrow {}^{\bullet}OH + H^+ + e^-. \quad (28)$$

In 2021, Jiang and coworkers [80] fabricated a magnetic p–n $Bi_2WO_6/CuFe_2O_4$, synthesized via a hydrothermal method, to remove tetracycline hydrochloride (TCH) from wastewater. They combined the heterogeneous photo-Fenton-like efficiency for water decontamination with $CuFe_2O_4$ (CFO), which has been widely studied because of its inverse spinel structure, characterized by a low toxicity, magnetism, and the active activation of H_2O_2 by Cu and Fe ions. In the mechanism of the photo-Fenton-like process, an inhibition of degradation efficiency was observed upon the addition of *n*-butanol, indicating that hydroxyl radicals were mainly responsible for the removal process. Moreover, when a known radical scavenger (KI) was added to the process, degradation efficiency reached 67%. Thus, it can be speculated that it was not the free radicals in the solution, but the surface-bound radicals that were mainly responsible for the degradation mechanism. When formic acid, *p*-benzoquinone (*p*-BQ), and $KBrO_3$ were added to the photo-Fenton-like process, a reduction in the efficiency was observed to a limited extent, and contributions of H^+, $O_2{}^-$, and e^- to the oxidation were found [80].

However, not only hydroxyl radicals play a role in the process. To investigate other radicals effectively contributing to the degradation, equivalent series resistance (ESR) tests were conducted. According to the studies, $O_2{}^{\bullet}$ was found in solution, presumably generated during the oxygen reduction. The generation of $O_2{}^{\bullet}$ in the presence of H_2O_2, involved in the reduction in Cu(II) and Fe(III), was also confirmed. Upon light irradiation, Fe(III)/Cu(II) is converted to Fe(II)/Cu(I), and hydroxyl radical generation takes place, as confirmed by the reduction in $O_2{}^{\bullet}$. The ROS results also confirmed the possibility of the generation of a large number of hydroxyl radicals under the influence of the synergistic excitation of light and H_2O_2 [80,101,107].

According to the results of electron spin resonance (ESR), the dominance of ${}^{\bullet}OH$ and $O_2{}^{\bullet}$ in the process was also confirmed by Wu et al. [106] in their study using 2D/2D FeNi-layered double hydroxide/bimetal–MOF nanosheets (2D/2D MOFs: FeNiLDH/BMNSs + H_2O_2 + Vis nanosheets) for an enhanced photo-Fenton degradation of antibiotics. Moreover, the production of ${}^{\bullet}OH$ was determined by detecting the enhanced PL signal [106].

To investigate the mechanism of the process on the surface of the magnetic p–n $Bi_2WO_6/CuFe_2O_4$, an X-ray photoelectron spectroscopy (XPS) spectrum analysis was carried out on a fresh and used 10BWO/CFO catalyst, revealing the possibility of the partial conversion of Cu(II) to Cu(I) and of Fe(III) to Fe(II). Thus, the authors also confirmed the involvement of Cu(II) and Fe(III) in the heterogeneous catalytic reaction [80]. Moreover, when the catalyst was introduced to UV light, holes were generated on its surface, resulting in a higher potential of hydroxyl radicals in the oxidation process. Jiang et al. [80] also noted that electrons of the BWO surface reduced the adsorption of O_2 with the generation of ${}^{\bullet}O^{2-}$.

However, not only ROS play an important role in the process. A crucial index to assess the performance of AOPs is the decomposition rate of H_2O_2 [108]. Wu et al. [106] observed that an increase in the amount of H_2O_2 in the process resulted in an increase in the degradation rate within the first 15 min of the process. This was due to the high reactivity of H_2O_2 and, as a result, its rapid degradation. However, a further change in the dose of H_2O_2 did not increase the catalytic activity. This was due to the reactions of H_2O_2 resulting in the conversion of $^{\bullet}OH$ to less reactive $^{\bullet}OOH$. Excess H_2O_2 could also compete with the antibiotic for active sites on the photocatalyst surface, decreasing the process efficiency. The authors also noted that H_2O_2 (5 mM) was completely decomposed after heating at 90 °C for 120 min. Additionally, they confirmed the synergistic effect of the FeNi-LDH/BMNSs photocatalyst and Vis on decomposing H_2O_2 into $^{\bullet}OH$ [106].

The mechanisms of modified Fenton processes using 2D materials, MXenes, or nanostructures appear to be very similar to those of the classical Fenton process [14], as well as its modification using a heterogeneous catalyst, light, or electrochemical modification. Due to their composite structure, the proportion of heterogeneous reactions on the catalyst surface increases. As a result, the pool of radicals and active sites increases, improving the process [68,80]. However, there are still problems to be solved in the process, such as the termination of hydroxyl radicals and the acidic environment needed to achieve better treatment results.

7. Potential Environment Applications and Efficiency of Degradation Process

The implementation of the process in the industry requires process optimization. In addition, the method of the degradation of pollutants must be effective. Moreover, this method should be suitable for the treatment of many different chemical compounds [109]. Very often, nonbiodegradable substances are characterized by their high toxicity [110–112]. This threat is mainly posed by industrial plants (e.g., pharmaceutical [110] and cosmetic plants, fertilizer production, paint and lacquer factories, etc.). Therefore, it is essential to choose an appropriate cleaning method among the various harmful compounds, obtaining the highest possible efficiency while using low amounts of reactants.

The formation of components with different catalytic properties is recognized as an efficient way to obtain AOP catalysts capable of inducing cascade reactions in the modified Fenton process. This raises the potential for the use of 2D compounds on an industrial scale.

The high efficiency of the process was evaluated by Cheng et al. [72]. In this study, under simulated sunlight irradiation (SSI), rhodamine B(RhB) decomposed very quickly in the presence of a material composed of microporous MXene monolayers embedded with Ti^{3+}-doped and TiO_2 nanodot–mpMXene/TiO_{2-x} NDs as the catalyst, along with low-dose H_2O_2 (0.7 mM). Results showed a 96% decrease in RhB molecules (30 mg·L^{-1}) in 10 min with a TOC removal of 55.4% at 1 h under these conditions [72].

Tao et al. [107] fabricated Fe-based metal–organic frameworks (Fe-MOFs) using the dielectric barrier discharge (DBD) plasma method with $FeSO_4 \cdot 7H_2O$ as the Fe precursor in a photo-Fenton-like process to degrade methyl orange (MO). The degradation reached 96.4% after 8 min in process conditions with a catalyst concentration of 1 g·L^{-1} at pH 3, 2 mL·L^{-1} H_2O_2, and a discharge voltage of 14.5 kV.

Because of the risk to human health and the aquatic environment, pharmaceuticals and personal care products (PPCPs) are pollutants of concern [10,113]. Not surprisingly, many scientists are focused on finding a universal and cost-effective method to degrade these compounds and remove them from the aquatic environment.

A high degradation efficiency was noted by Ma et al., as already cited above [68], in a study on ranitidine catalytic degradation using nanoscale zero-valent iron particles, Ti_3C_2-based MXene nanosheets, and nZVI@Ti3C2 as a catalyst (a concentration of 0.5 g·L^{-1} in a mass ratio of 3:1 ZVI to Ti_3C_2-based MXene) in a modified Fenton-like process. They studied the degradation efficiency of ranitidine (at a concentration of 5 mg·L^{-1}) at temperatures of 15, 20, 25, 30, and 35 °C (pH 4.5, 0.5 mM H_2O_2). They noted a clear dependence of the iron-based process efficiency on the temperature. With an increase in temperature,

a marked increase in ranitidine degradation was observed with the reaction speed improving from 3.89×10^{-2} to 7.68×10^{-2} min^{-1}. Using the abovementioned concentrations of substrate and catalyst, under acidic conditions (pH 4.5) at a temperature of 25 °C, the degradation of ranitidine and total organic carbon (TOC) reached 91.1% and 63.3%, respectively, after 30 min of running the process.

Ye et al. [101] attempted to treat urban wastewater and evaluated the morphological, physicochemical, and photocatalytic properties of Fe-MOFs with 2,2′-bipyridine-5,5′-dicarboxylate (Fe-bpydc) during a photoelectro-Fenton process under UVA (ultraviolet A; wavelength from 320 to 400 nm) and visible-light irradiation. The process took 90 min at a temperature of 25 °C, with an initial pH of 7.4 (concentrations of naproxen, fluoxetine, bisphenol A, and bezafibrate were equal to 10 $mg \cdot L^{-1}$ each, while the concentration of Fe-bpydc was equal to 0.05 $g \cdot L^{-1}$) in an IrO_2/air diffusion cell at 100 mA with a 150 W Xe lamp. After the process, the amounts of naproxen, fluoxetine, and bisphenol A decreased by 93%, 85%, and 78%, respectively, while the amount of bezafibrate decreased by 61%, confirming the ability to achieve the quick and complete removal of organic micropollutants using a very small amount of catalyst. Moreover, this confirmed the great potential of 2D material modifications to improve mass transport, increase the availability of catalyst active sites, or enhance reactive radical generation reactions in Fenton-like processes [101].

A 2D MOF was used as a catalyst by Wu et al. [106] in their study on antibiotic degradation. The high efficiency of the 2D/2D FeNi-layered double hydroxide/bimetal–organic framework nanosheets (FeNi-LDH/BMNSs + H_2O_2 + Vis system) was demonstrated. A 95.76% degradation of tetracycline hydrochloride (TCH) at a concentration of 20 $mg \cdot L^{-1}$ was achieved in 60 min under visible-light irradiation ($\lambda > 420$ nm, 500 W lamp), using a 30 wt.% H_2O_2 and 0.2 $g \cdot L^{-1}$ catalyst, at a pH of 3.07. The degradation of TCH via the photo-Fenton process using the FeNi-LDH/BMNS catalyst was also verified in different water matrices (DI water, river water, lake water, and tap water), achieving TCH degradation rates of 94.76%, 78.23%, 62.54%, and 68.69%, respectively. The authors also implemented this system for other antibiotics. Degradation efficiencies of 88%, 73%, 78%, and 79% were obtained for oxycycline, levofloxacin, norfloxacin, and doxycycline, respectively [106]. These examples highlight the wide applicability of 2D compounds.

In addition, Ihsanullah et al. [114] confirmed the adsorption–reduction properties of MXenes and MXene-based composites for numerous pollutants present in water (e.g., heavy metals, radionuclides, or dyes). Their study confirmed the potential of using MXenes in the modified Fenton process to degrade these compounds; thus, being effective in wastewater treatment or water purification.

The efficiency of the process is affected by many factors such as the pH, type and dose of substances present in the wastewater, dose and ratio of reactants, reaction time, and temperature. A change in any of these parameters can affect the efficiency of the entire process. Moreover, depending on the process modification used, further parameters may appear (e.g., wavelength in photo-modification or current in electro-modification). These parameters also contribute to the final process efficiency. Examples of the effect of changes in process parameters are given below [103].

Cui et al. [67] used different pH values (pH = 3, 5, 7, 9, and 11) in their study on the Fenton-like degradation of methylene blue (MB) using composites of Ti_3C_2 MXene and Fe_3O_4 magnetic nanoparticles (MX-MNPs). They observed a decrease in the degradation efficiency with an increase in pH (H_2O_2 concentration of 50 $mmol \cdot L^{-1}$ and catalyst concentration of 0.5 $g \cdot L^{-1}$). The degradation of MB decreased from 96% to 72% at pH values of 3–11, respectively [67].

The dosage of pollutants was studied by Jiang et al. [80] in the photo-Fenton degradation of tetracycline hydrochloride (TCH) using the magnetic p–n $Bi_2WO_6/CuFe_2O_4$ (10BWO/CFO) as a catalyst. They used four different TCH concentrations (10.0, 20.0, 30.0, and 40.0 $mg \cdot L^{-1}$) at a pH of 4.0 (10.0 $mmol \cdot L^{-1}$ H_2O_2 and 1.0 $g \cdot L^{-1}$ catalyst). They observed that the efficiency of the process depended on the TCH concentration. When the concentration was 10.0 $mg \cdot L^{-1}$, the TCH degradation reached almost 100% after 5 min.

However, with a concentration of 40.0 mg·L^{-1}, the maximal degradation of TCH decreased to 76% within 20 min [80].

On the other hand, Wang et al. [102] investigated the effect of an H_2O_2 dose and catalyst on the process efficiency in the photo-Fenton-like degradation of chloroquine phosphate (CQ), at a concentration of 10 mg·L^{-1}, using BUC-21(Fe) ($C_{54.5}H_{45}Fe_2N_8O_{13}$) at a concentration of 15 mg·L^{-1} (pH = 5.0). Upon increasing the H_2O_2 dosage from 5 µL to 15 µL, the removal of CQ also increased from 76.3% to 100% within 30 min. A further increase to 20 µL reduced the efficiency of the process. The corresponding degradation rate (*k* values) increased from 0.0413 to 0.1162 min^{-1} and then decreased to 0.1101 min^{-1} upon increasing the H_2O_2 dosage to 20 µL [87]. They conducted their study using a modification of the Fenton process with UV light (10 W LED UV light). They observed a decrease in the degradation efficiency with an increase in the wavelength. Under UV light at a wavelength of 365 nm, the degradation of CQ reached 100%. Upon increasing the wavelength to 420, 485, 520, and 630 nm, the degradation of CQ reached 95%, 93%, 91%, and 82%, respectively [102].

For the process of internal micro-electrolysis-enhanced heterogeneous electro-Fenton degradation of sulfamethazine catalyzed by a core–shell-structured hybrid octahedron containing a nanoparticle core (Fe/Fe_3C) and a graphitized porous carbon (PC) shell (Fe/Fe_3C@PC), Du et al. [115] studied the effect of the amount of catalyst on process efficiency. With an increase in catalyst dosage from 25 to 75 mg·L^{-1}, the value of *k* increased from 0.036 to 0.088 min^{-1}. However, a further increase to 100 mg·L^{-1} led to a reduction in *k* to 0.072 min^{-1}. The authors determined similar observations when studying the effect of current on the reaction. When the current increased from 5.0 mA to 25.0 mA, the value of *k* also increased from 0.036 to 0.086 min^{-1}. However, a further increase in current to 45.0 mA resulted in a decrease in *k* to 0.053 min^{-1} [115].

In the studies mentioned above, the dependence of the process running time on the values of individual parameters could be observed. Usually, the fastest process occurred within the first 5–20 min with a process efficiency above 90%, before slowing down. Typically, the reaction was accelerated using the optimal level of individual parameters, which increased the efficiency of the process [87,102,115].

The structures of compounds and their degradation of various harmful substances highlight their applicability for urban or industrial wastewater treatment. The information provided in the above examples has been successively confirmed and extended by other researchers studying the use of 2D compounds, including MXenes, in the photo-Fenton-like process. A multitude of studies performed on laboratory-synthesized matrices, confirming the high efficiency of treatment, should attract the attention of research groups and encourage the implementation of modified processes on real matrices from industrial plants.

8. Stability and Recyclability

One of the most critical properties of used catalysts in practical application is their recyclability and stability. In times of increasing environmental awareness and, thus, attempts to reduce the negative impact of human activity on the environment, recyclability is a topic that appears in almost every field. The possibility of reusing materials undoubtedly reduces the use of natural and synthetically obtained resources. This, in turn, translates into a reduction in waste from any process. Another significant aspect is the financial benefit. Appropriately selected methods of recyclability allow reducing, e.g., the costs of energy consumption or the purchase of fresh material [116].

Closely related to recyclability is material stability. A stable material means an increased reusability, which can influence the efficiency of the process. Therefore, in work involving experimental materials, newly synthesized or applicable to a process for the first time, researchers explored the mechanism of action underlying the process and the stability of the compound on which they based their research.

Previous work has mostly confirmed the rather high stability of 2D compounds and the possibility of multiple reuses with a high efficiency when carrying out the degradation

process. For example, in Cheng et al.'s study [72], after 10 cycles, the photo-Fenton reaction over mp-MXene/TiO_{2-x} NDs as a catalyst in the process of rhodamine degradation showed a similar efficiency to the first cycle of RhB degradation.

Luo et al. [117] studied the degradation of a model dye (methylene blue (MB)). They synthesized Co_3O_4 particle-modified MXene (Mxene-Co_3O_4) nanocomposites. The degradation process was carried out using an MB concentration of 5 mg·L^{-1}, with 10 mg·L^{-1} of catalyst and 15 mL of H_2O_2 (30%) at room temperature. After eight cycles, the MB removal rate was maintained at 92.37%.

Slightly fewer cycles were carried out by Tao et al. [107], who created Fe-based metal–organic frameworks (Fe-MOFs) using the dielectric barrier discharge (DBD) plasma method and $FeSO_4 \cdot 7H_2O$. They carried out six cycles of degradation, maintaining a more than 89% degradation efficiency under the following process conditions: discharge voltage, 14.5 kV; reaction time, 100 min; pH, 3; reactant concentration, 12 g·L^{-1}.

As already mentioned above, Cui et al. [67] prepared composites of Ti_3C_2 MXene Fe_3O_4 magnetic nanoparticles (MX-MNPs) for methylene blue (MB) degradation, achieving a high process efficiency after five cycles of running the process. After 1 min, the degradation efficiency decreased from 96% (first cycle) to 84.36% (second cycle), 83.64% (third cycle), 79.73% (fourth cycle), and 71.54% (fifth cycle). The process parameters were as follows: pH, 3; concentration of catalyst, 0.5 g·L^{-1}; concentration of H_2O_2, 50 mmol·L^{-1}.

Ma et al. [68] obtained high catalytic activity after five repetitions of ranitidine (5 mg·L^{-1}) degradation using magnetic nanoscale zero-valent iron (nZVI)@Ti_3C_2-based MXene nanosheets (nZVI@Ti_3C_2) at a concentration of 0.5 g·L^{-1}, with 0.5 mM H_2O_2, at a temperature of 25 °C and pH of 4.5. Ultrapure water without any further treatment and HCl was used to recycle the catalyst. When ultrapure water was used, a marked decrease in the process efficiency was observed from 91.4% to 74.1% after five cycles. HCl was found to be the optimal catalyst treatment with a decrease in efficiency from 92.5% to 86.1%. The tests proved that the reduction in the efficiency and recyclability of the process was due to the blocking of active sites of the catalyst. Due to the magnetic properties of the catalyst, it was possible to easily separate it from the rest of the solution, which affected its recyclability. Moreover, nZVI@Ti_3C_2 could be well dispersed, and it remained in suspension for 3 days.

A similar effect was obtained by Ihsanullah et al. [114]. After five cycles of adsorption–desorption, the degradation efficiency slightly decreased from 185.63 mg/g to 167.2 mg/g. The authors regenerated the delaminated 2D titanium carbide MXene ($Ti_3C_2T_x$-DL) using 0.5 mol/L thiourea after the absorption of Pd^{2+}. This provided excellent desalting performance compared to traditional eluting agents such as HCl or HNO_3 [114].

Wu et al. [106] noted an exceptional cycle stability toward the degradation of tetracycline hydrochloride (TCH) using FeNi-LDH/BMNSs as a catalyst. In addition, the TOC removal rate was 48.98% after four cycles. FeNi-LDH/BMNS was recovered after the first start-up. Moreover, the results indicated its structural stability during the cycle test [106].

The Fe-based 2D MOF showed less recyclability in Ye et al.'s [101] study. After three runs of 90 min using the same Fe-MOF with 2,2′-bipyridine-5,5′-dicarboxylate (Febpydc) in a concentration of 0.05 g·L^{-1}, the maximum efficiency achieved in the UV/Vis PEF process (IrO_2/air-diffusion cell at 100 mA, pH 5.1, and 25 °C) was 30%. Regarding the stability of the compound, it is known that, when MOFs react in aqueous media, they lose crystallinity, causing phase changes that can eventually lead to the destruction of the porous structure or ultimate decomposition. Therefore, bipyridine was used in this study because of its strong binding affinity to Fe (II) ions and resistance to hydroxyl radicals. As a result, no significant changes in the crystallinity and structure of the catalyst were observed, and partial deactivation was attributed to the blocking of the more prominent active sites [101].

On the other hand, a spectacular result was achieved by Jiang et al. [80]. They studied the degradation of tetracycline hydrochloride (TCH) in a photo-Fenton process using the magnetic p–n $Bi_2WO_6/CuFe_2O_4$ (10BWO/CFO) as a catalyst. The degradation efficiency was decreased by only 3% after four cycles. This effect demonstrates the excellent stability

of the prepared catalyst. The process conditions were as follows: H_2O_2, 10.0 mmol·L^{-1}; pH, 4.0; catalyst dosage, 1.0 g·L^{-1}; dosage of TCH, 20.0 mg·L^{-1}.

The stability of the compound and its reusability are features identified by researchers for improving the process efficiency. The possibility of easy separation of the catalyst and its reuse, even multiple times, while maintaining a high efficiency of the process, contributes to a reduction in the financial cost for its implementation, as well as a reduction in postprocessing waste (sludge). The properties of 2D compounds and their modifications are relatively novel topics in the literature. Therefore, depending on the particular materials or modifications introduced, 2D compounds exhibit different properties. In the studies cited above, researchers observed satisfactory effects when reusing (even 10 times [72], with an average efficiency of about 80%) different 2D materials in processes [68,72,101,106,107,114]. The promising degradation results achieved after multiple process cycles confirmed the previous reports of versatility [76–78,91–93,107,117]. However, knowledge of the properties of 2D materials and their modifications should be further developed in order to find a material that incorporates as many properties as possible for the most effective purification process.

9. Toxicity of Process

Nanotechnology has many advantages over time-honored environmental solutions [102,103,118]. Thus, reports regarding their potential application in different fields have grown exponentially in the last decade [119]. Despite the superior potential of 2D nanomaterials in environmental processes, one needs to assume their possible release into natural ecosystems. Therefore, worldwide concerns regarding their toxicity have been raised [120–123]. The impact of 2D nanomaterials on living organisms includes physical and biochemical interactions [124]. The most frequently described nanoblade mechanism concerns cell damage caused by the sharp edges of 2D nanoflakes [125–129]. Additionally, many studies have confirmed the induction of oxidation stress due to the generation of reactive oxygen species (ROS) in the presence of 2D nanomaterials [130–133]. Both mechanisms may also simultaneously impact the fauna and flora, resulting in an inconsistent cell membrane, leakage of the cytoplasm and organelles, DNA and protein damage, and metabolism disruption [50,134–136].

Moreover, 2D nanomaterials may affect organisms not only at the point of deposition, but migration toward higher elements of trophic chains is also possible. Next, the toxicity may increase via a process called biomagnification, in which toxins are passed from one trophic level to another. Consequently, an increase in the concentration within a food web is observed [137].

In the Fenton process, the degradation of pollutants is achieved. However, the decomposition is incomplete, and many toxic byproducts may be generated [138–140]. Therefore, studies regarding the potential impact of the process on living organisms need to include the toxicity of the catalyst and postprocessing effluent.

A complex toxicity assessment was performed by Jiang et al. [80]. They compared dark and photo-Fenton reactions in the degradation of tetracycline hydrochloride (TCH) using $Bi_2WO_6/CuFe_2O_4$ (BWO/CFO), studying the toxicity of the utilized catalysts and obtained effluent. Interestingly, despite the applied dose, BWO/CFO did not disturb the growth of *E. coli* and *S. aureus*. Furthermore, they found 19 degradation products of TCH due to the treatment, which they checked for potential toxicity. Results obtained for fathead minnows and *Daphnia magna* suggested that most byproducts were less toxic than TCH. In addition, the mutagenicity of the effluent was not confirmed, whereas TCH was rated as mutagenic [80].

Liu et al. [93] utilized Fe (III)-based metal–organic frameworks in the photo-Fenton process. Furthermore, they studied effluent intermediates and their potential interference with the *E. coli* metabolism. They found that, due to the degradation of tris-(2-chloroisopropyl) phosphate, carboxylated, dechlorinated, and hydroxylated products were generated. Additional observations of metabolomics of *E. coli* performed in the presence of the obtained byproducts confirmed their slight toxic influence [79]. Wang et al. [102] also reported the application of 2D Fe-based MOF sheets in the photo-Fenton process. They found the high

efficiency of such a system in the degradation of chloroquine phosphate. Interestingly, they proposed a degradation pathway, where, even though the studied organic contaminants degraded into small molecules, their toxicity was not detected [87].

Contrary to previous reports, Wu et al. [141] studied Fe (II) ion-doped $Ti_3C_2T_x$ MXenes in Fenton-based anticancer therapy. They found that reactive oxide species (ROS) were generated in the presence of the catalyst. Moreover, the studied MKN45 cells released glutathione, which suggests antioxidant action and the induction of oxidative stress in the presence of the MXene-based catalyst [141,142]. Liang et al. [65] also combined $Ti_3C_2T_x$ MXene and iron oxide nanoparticles as nanocatalysts in Fenton-based cancer therapy. Interestingly, such a system without NIR laser irradiation showed negligible cytotoxicity toward 4T1 murine mammary carcinoma cells. However, due to the additional irradiation, they observed the generation of hydroxyl radicals and cytotoxicity caused by localized hyperthermia. Furthermore, the studies performed on nude mice showed a tendency of MXene-based nanocomposites to accumulate in the spleen and liver, which suggests an uptake by the reticuloendothelial system [65].

Two-dimensional nanostructures offer several potential benefits for AOPs, such as a high potential in organic pollutant degradation, superior efficiency in the face of ordinary catalysts, reusability, and cost-effectiveness. In the excitement of the obtained results, scientists often tend to forget about a crucial aspect of every environmental process: toxicity. It can manifest not only in the generation of potentially harmful compounds present in the effluent, but also in the negative bioactivity of the catalyst itself. The complexity of ecosystems, migration of toxicants, their biotransformation, the potential of accumulation in different components of ecological systems, and the alternating ability of various species to metabolize them raise a great challenge for the future. Therefore, more detailed investigation schemes regarding every aspect of the application of 2D nanostructures and AOPs in the environment need to be developed and explored.

10. Summary and Future Perspective

This review focused on the removal efficiency of substances from wastewater or other matrices characterized by nonbiodegradable substances. Two-dimensional materials, including MXenes, have shown a high catalytic activity toward various pollutants. Their appropriate modification confers them excellent contaminant selectivity. Moreover, MXenes and their modification also exhibit strong adsorption and reduction properties, allowing them to be successfully used for the removal of heavy metals, dyes, pharmaceuticals, and radionuclides. Studies also confirmed the high stability of 2D materials, as well as their potential for regeneration and reuse after adsorption.

Despite the many desirable features of 2D materials, MXenes, and nanostructures, the use of these materials in processes is not without drawbacks. Disadvantages of using these materials arise from an incomplete understanding of their mechanism of action and different environmental impacts depending on the compound. Moreover, these materials have only been synthesized in laboratory conditions. Therefore, their acquisition is costly.

A key component of future research is to understand the exact mechanism of the compounds in the treatment process to increase their efficiency and eliminate the disadvantages of the treatment process. Moreover, the development and popularization of a method for the obtainment of 2D catalysts with implementations on an industrial scale would reduce production costs.

Using a modified Fenton process with a 2D catalyst for wastewater treatment would help reduce the environmental risk caused by nonbiodegradable substances. Due to the high degradation of harmful compounds in model wastewaters, it is also worthwhile to focus on the study of urban or industrial wastewaters. Previous reports on the use of process modifications in real matrices (polluted flowing waters or lakes) seem to be a promising perspective for industrial wastewater treatment.

The Fenton AOP involves the nonselective oxidation of compounds in solution. Modifications of the process are intended to increase its efficiency, mainly by increasing the

generation of hydroxyl radicals, reducing the risk of cross-quenching reactions, and eliminating the disadvantages of the system.

Author Contributions: D.Ś. prepared the abstract, introduction, mechanism of the photo-Fenton process with 2D structures, summary and future perspective, efficiency and application, stability, and recyclability. D.B. prepared the 2D structures and bibliography. M.J. prepared the toxicity. A.J., J.B. and P.M. coordinated and supervised the preparation of the manuscript and corrected the original manuscript. All authors have read and agreed to the published version of the manuscript.

Funding: D.B. acknowledges funding from the National Science Centre, within the framework of the research project 'OPUS-16' (UMO-2018/31/B/ST3/03758). M.J. acknowledges funding from the National Science Centre, within the framework of the research project 'OPUS-18' (UMO-2019/35/B/ST5/02538). D.Ś., D.B., and M.J. also additionally acknowledge financial support from the ID-UB project (Scholarship Plus programme).

Conflicts of Interest: The authors declare no conflict of interest.

References

1. de Oliveira Neto, G.C.; Correia, J.M.F.; Silva, P.C.; de Oliveira Sanches, A.G.; Lucato, W.C. Cleaner Production in the textile industry and its relationship to sustainable development goals. *J. Clean. Prod.* **2019**, *228*, 1514–1525. [CrossRef]
2. Tekin, H.; Bilkay, O.; Ataberk, S.S.; Balta, T.H.; Ceribasi, I.H.; Sanin, F.D.; Dilek, F.B.; Yetis, U. Use of Fenton oxidation to improve the biodegradability of a pharmaceutical wastewater. *J. Hazard. Mater.* **2006**, *136*, 258–265. [CrossRef] [PubMed]
3. Dominguez, D.; Gujer, W. Evolution of a wastewater treatment plant challenges traditional design concepts. *Water Res.* **2006**, *40*, 1389–1396. [CrossRef] [PubMed]
4. Ajiboye, T.O.; Oyewo, O.A.; Onwudiwe, D.C. Simultaneous removal of organics and heavy metals from industrial wastewater: A review. *Chemosphere* **2021**, *262*, 128379. [CrossRef] [PubMed]
5. Eggen, R.I.L.; Hollender, J.; Joss, A.; Schärer, M.; Stamm, C. Reducing the Discharge of Micropollutants in the Aquatic Environment: The Benefits of Upgrading Wastewater Treatment Plants. *Environ. Sci. Technol.* **2014**, *48*, 7683–7689. [CrossRef]
6. de Andrade, P.M.; Dufrayer, C.R.; Ionashiro, E.Y.; de Brito, N.N. The use of metallurgical waste for heterogeneous photo Fenton-Like treatment of cosmetic effluent. *J. Environ. Chem. Eng.* **2020**, *8*, 104148. [CrossRef]
7. Cai, Q.Q.; Lee, B.C.Y.; Ong, S.L.; Hu, J.Y. Fluidized-bed Fenton technologies for recalcitrant industrial wastewater treatment–Recent advances, challenges and perspective. *Water Res.* **2021**, *190*, 116692. [CrossRef]
8. Zajda, M.; Aleksander-Kwaterczak, U. Wastewater Treatment Methods for Effluents from the Confectionery Industry—An Overview. *J. Ecol. Eng.* **2019**, *20*, 293–304. [CrossRef]
9. Ghime, D.; Ghosh, P. Advanced Oxidation Processes: A Powerful Treatment Option for the Removal of Recalcitrant Organic Compounds. In *Advanced Oxidation Processes: Applications, Trends, and Prospects*; IntechOpen: London, UK, 2020; pp. 1–12.
10. Bogacki, J.; Naumczyk, J.; Marcinowski, P.; Kucharska, M. Oczyszczanie ścieków kosmetycznych metodami fizykochemicznymi i chemicznymi. *Chemik* **2011**, *65*, 94–97.
11. Deng, Y.; Zhao, R. Advanced Oxidation Processes (AOPs) in Wastewater Treatment. *Curr. Pollut. Rep.* **2015**, *1*, 167–176. [CrossRef]
12. Shahedi, A.; Darban, A.K.; Taghipour, F.; Jamshidi-Zanjani, A. A review on industrial wastewater treatment via electrocoagulation processes. *Curr. Opin. Electrochem.* **2020**, *22*, 154–169. [CrossRef]
13. Crini, G.; Lichtfouse, E. Advantages and disadvantages of techniques used for wastewater treatment. *Environ. Chem. Lett.* **2019**, *17*, 145–155. [CrossRef]
14. Ribeiro, J.P.; Nunes, M.I. Recent trends and developments in Fenton processes for industrial wastewater treatment—A critical review. *Environ. Res.* **2021**, *197*, 110957. [CrossRef] [PubMed]
15. Pereira, M.C.; Oliveira, L.C.A.; Murad, E. Iron oxide catalysts: Fenton and Fentonlike reactions—A review. *Clay Miner.* **2012**, *47*, 285–302. [CrossRef]
16. Bogacki, J.; Marcinowski, P.; Bury, D.; Krupa, M.; Ścieżyńska, D.; Prabhu, P. Magnetite, Hematite and Zero-Valent Iron as Co-Catalysts in Advanced Oxidation Processes Application for Cosmetic Wastewater Treatment. *Catalysts* **2020**, *11*, 9. [CrossRef]
17. Bogacki, J.; Marcinowski, P.; Zapałowska, E.; Maksymiec, J.; Naumczyk, J. Cosmetic wastewater treatment by the ZVI/H_2O_2 process. *Environ. Technol.* **2017**, *38*, 2589–2600. [CrossRef]
18. Marcinowski, P.; Bury, D.; Krupa, M.; Ścieżyńska, D.; Prabhu, P.; Bogacki, J. Magnetite and Hematite in Advanced Oxidation Processes Application for Cosmetic Wastewater Treatment. *Processes* **2020**, *8*, 1343. [CrossRef]
19. Muszyński, A.; Marcinowski, P.; Maksymiec, J.; Beskowska, K.; Kalwarczyk, E.; Bogacki, J. Cosmetic wastewater treatment with combined light/Fe0/H2O2 process coupled with activated sludge. *J. Hazard. Mater.* **2019**, *378*, 120732. [CrossRef]
20. Poza-Nogueiras, V.; Rosales, E.; Pazos, M.; Sanromán, M.Á. Current advances and trends in electro-Fenton process using heterogeneous catalysts—A review. *Chemosphere* **2018**, *201*, 399–416. [CrossRef]
21. Carey, J.H. An Introduction to Advanced Oxidation Processes (AOP) for Destruction of Organics in Wastewater. *Water Qual. Res. J.* **1992**, *27*, 1–22. [CrossRef]

22. Iuga, C.; Campero, A.; Vivier-Bunge, A. Antioxidant vs. prooxidant action of phenothiazine in a biological environment in the presence of hydroxyl and hydroperoxyl radicals: A quantum chemistry study. *RSC Adv.* **2015**, *5*, 14678–14689. [CrossRef]
23. Valange, S.; Védrine, J.C. General and Prospective Views on Oxidation Reactions in Heterogeneous Catalysis. *Catalysts* **2018**, *8*, 483. [CrossRef]
24. Babuponnusami, A.; Muthukumar, K. A review on Fenton and improvements to the Fenton process for wastewater treatment. *J. Environ. Chem. Eng.* **2014**, *2*, 557–572. [CrossRef]
25. Sriprom, P.; Krobthong, W.; Assawasaengrat, P. Investigation of important parameters for Photo-Fenton degradation of methyl orange over Fe/TiO_2 catalyst. *Energy Rep.* **2020**, *6*, 731–736. [CrossRef]
26. Sabour, M.R.; Lak, M.G.; Rabbani, O. Evaluation of the main parameters affecting the Fenton oxidation process in municipal landfill leachate treatment. *Waste Manag. Res.* **2011**, *29*, 397–405. [CrossRef]
27. Allendorf, M.D.; Stavila, V. Crystal engineering, structure–function relationships, and the future of metal-organic frameworks. *CrystEngComm* **2015**, *17*, 229–246. [CrossRef]
28. Dong, J.; Zhao, Y.; Zhao, R.; Zhou, R. Effects of pH and particle size on kinetics of nitrobenzene reduction by zero-valent iron. *J. Environ. Sci.* **2010**, *22*, 1741–1747. [CrossRef]
29. Liu, Y.; Zhao, Y.; Wang, J. Fenton/Fenton-like processes with in-situ production of hydrogen peroxide/hydroxyl radical for degradation of emerging contaminants: Advances and prospects. *J. Hazard. Mater.* **2021**, *404*, 124191. [CrossRef]
30. Xiao, K.; Pei, K.; Wang, H.; Yu, W.; Liang, S.; Hu, J.; Hou, H.; Liu, B.; Yang, J. Citric acid assisted Fenton-like process for enhanced dewaterability of waste activated sludge with in-situ generation of hydrogen peroxide. *Water Res.* **2018**, *140*, 232–242. [CrossRef]
31. Sheng, H.; Janes, A.N.; Ross, R.D.; Kaiman, D.; Huang, J.; Song, B.; Schmidt, J.R.; Jin, S. Stable and selective electrosynthesis of hydrogen peroxide and the electro-Fenton process on $CoSe_2$ polymorph catalysts. *Energy Environ. Sci.* **2020**, *13*, 4189–4203. [CrossRef]
32. Yang, H.; Shi, B.; Wang, S. Fe Oxides Loaded on Carbon Cloth by Hydrothermal Process as an Effective and Reusable Heterogenous Fenton Catalyst. *Catalysts* **2018**, *8*, 207. [CrossRef]
33. Yu, T.; Breslin, C.B. Graphene-Modified Composites and Electrodes and Their Potential Applications in the Electro-Fenton Process. *Materials* **2020**, *13*, 2254. [CrossRef] [PubMed]
34. Zhang, M.-H.; Dong, H.; Zhao, L.; Wang, D.-X.; Meng, D. A review on Fenton process for organic wastewater treatment based on optimization perspective. *Sci. Total Environ.* **2019**, *670*, 110–121. [CrossRef] [PubMed]
35. Ebrahiem, E.E.; Al-Maghrabi, M.N.; Mobarki, A.R. Removal of organic pollutants from industrial wastewater by applying photo-Fenton oxidation technology. *Arab. J. Chem.* **2017**, *10*, S1674–S1679. [CrossRef]
36. Lan, H.; Wang, A.; Liu, R.; Liu, H.; Qu, J. Heterogeneous photo-Fenton degradation of acid red B over Fe_2O_3 supported on activated carbon fiber. *J. Hazard. Mater.* **2014**, *285*, 167–172. [CrossRef]
37. Velichkova, F.; Delmas, H.; Julcour, C.; Koumanova, B. Heterogeneous fenton and photo-fenton oxidation for paracetamol removal using iron containing ZSM-5 zeolite as catalyst. *AIChE J.* **2017**, *63*, 669–679. [CrossRef]
38. Giannakis, S. A review of the concepts, recent advances and niche applications of the (photo) Fenton process, beyond water/wastewater treatment: Surface functionalization, biomass treatment, combatting cancer and other medical uses. *Appl. Catal. B Environ.* **2019**, *248*, 309–319. [CrossRef]
39. He, H.; Zhou, Z. Electro-Fenton process for water and wastewater treatment. *Crit. Rev. Environ. Sci. Technol.* **2017**, *47*, 2100–2131. [CrossRef]
40. Kang, M.-H.; Lee, D.; Sung, J.; Kim, J.; Kim, B.H.; Park, J. 2.04-Structure and Chemistry of 2D Materials. In *Comprehensive Nanoscience and Nanotechnology*, 2nd ed.; Andrews, D.L., Lipson, R.H., Nann, T., Eds.; Academic Press: Cambridge, MA, USA, 2019; pp. 55–90.
41. Wang, Z.; Zhu, W.; Qiu, Y.; Yi, X.; Bussche, A.V.D.; Kane, A.; Gao, H.; Koski, K.; Hurt, R. Biological and environmental interactions of emerging two-dimensional nanomaterials. *Chem. Soc. Rev.* **2016**, *45*, 1750–1780. [CrossRef]
42. Zhao, Y.; Zhang, S.; Shi, R.; Waterhouse, G.I.N.; Tang, J.; Zhang, T. Two-dimensional photocatalyst design: A critical review of recent experimental and computational advances. *Mater. Today* **2020**, *34*, 78–91. [CrossRef]
43. Xu, J.; Li, W.; Hou, Y. Two-Dimensional Magnetic Nanostructures. *Trends Chem.* **2020**, *2*, 163–173. [CrossRef]
44. Anichini, C.; Czepa, W.; Pakulski, D.; Aliprandi, A.; Ciesielski, A.; Samorì, P. Chemical sensing with 2D materials. *Chem. Soc. Rev.* **2018**, *47*, 4860–4908. [CrossRef] [PubMed]
45. Li, X.; Bai, Y.; Shi, X.; Su, N.; Nie, G.; Zhang, R.; Nie, H.; Ye, L. Applications of MXene ($Ti_3C_2T_x$) in photocatalysis: A review. *Mater. Adv.* **2021**, *2*, 1570–1594. [CrossRef]
46. Tiwari, S.K.; Sahoo, S.; Wang, N.; Huczko, A. Graphene research and their outputs: Status and prospect. *J. Sci. Adv. Mater. Devices* **2020**, *5*, 10–29. [CrossRef]
47. Katsnelson, M.I. Graphene: Carbon in two dimensions. *Mater. Today* **2007**, *10*, 20–27. [CrossRef]
48. Mas-Ballesté, R.; Navarro, C.; Zamora, F. 2D materials: To graphene and beyond. *Nanoscale* **2011**, *3*, 20–30. [CrossRef] [PubMed]
49. Szuplewska, A.; Kulpińska, D.; Jakubczak, M.; Dybko, A.; Chudy, M.; Olszyna, A.; Brzózka, Z.; Jastrzębska, A.M. The 10th anniversary of MXenes: Challenges and prospects for their surface modification toward future biotechnological applications. *Adv. Drug Deliv. Rev.* **2022**, *182*, 114099. [CrossRef]
50. Jakubczak, M.; Szuplewska, A.; Rozmysłowska-Wojciechowska, A.; Rosenkranz, A.; Jastrzębska, A.M. Novel 2D MBenes—Synthesis, Structure, and Biotechnological Potential. *Adv. Funct. Mater.* **2021**, *31*, 2103048. [CrossRef]

51. Naguib, M.; Kurtoglu, M.; Presser, V.; Lu, J.; Niu, J.; Heon, M.; Hultman, L.; Gogotsi, Y.; Barsoum, M.W. Two-Dimensional Nanocrystals Produced by Exfoliation of Ti_3AlC_2. *Adv. Mater.* **2011**, *23*, 4248–4253. [CrossRef]
52. Khan, R.; Andreescu, S. MXenes-Based Bioanalytical Sensors: Design, Characterization, and Applications. *Sensors* **2020**, *20*, 5434. [CrossRef]
53. Guo, X.; Zhang, X.; Zhao, S.; Huang, Q.; Xue, J. High adsorption capacity of heavy metals on two-dimensional MXenes: An ab initio study with molecular dynamics simulation. *Phys. Chem. Chem. Phys.* **2016**, *18*, 228–233. [CrossRef]
54. Lim, G.P.; Soon, C.F.; Jastrzębska, A.M.; Ma, N.L.; Wojciechowska, A.R.; Szuplewska, A.; Omar, W.I.W.; Morsin, M.; Nayan, N.; Tee, K.S. Synthesis, characterization and biophysical evaluation of the 2D Ti_2CT_x MXene using 3D spheroid-type cultures. *Ceram. Int.* **2021**, *47*, 22567–22577. [CrossRef]
55. Shekhirev, M.; Shuck, C.E.; Sarycheva, A.; Gogotsi, Y. Characterization of MXenes at every step, from their precursors to single flakes and assembled films. *Prog. Mater. Sci.* **2021**, *120*, 100757. [CrossRef]
56. Ihsanullah, I. Potential of MXenes in Water Desalination: Current Status and Perspectives. *Nano-Micro Lett.* **2020**, *12*, 72. [CrossRef] [PubMed]
57. Jakubczak, M.; Karwowska, E.; Rozmysłowska-Wojciechowska, A.; Petrus, M.; Woźniak, J.; Mitrzak, J.; Jastrzębska, A.M. Filtration Materials Modified with 2D Nanocomposites—A New Perspective for Point-of-Use Water Treatment. *Materials* **2021**, *14*, 182. [CrossRef]
58. Szuplewska, A.; Rozmysłowska-Wojciechowska, A.; Poźniak, S.; Wojciechowski, T.; Birowska, M.; Popielski, M.; Chudy, M.; Ziemkowska, W.; Chlubny, L.; Moszczyńska, D.; et al. Multilayered stable 2D nano-sheets of Ti_2NT_x MXene: Synthesis, characterization, and anticancer activity. *J. Nanobiotechnol.* **2019**, *17*, 114. [CrossRef]
59. Pang, J.; Mendes, R.G.; Bachmatiuk, A.; Zhao, L.; Ta, H.Q.; Gemming, T.; Liu, H.; Liu, Z.; Rummeli, M.H. Applications of 2D MXenes in energy conversion and storage systems. *Chem. Soc. Rev.* **2019**, *48*, 72–133. [CrossRef]
60. Morales-García, Á.; Calle-Vallejo, F.; Illas, F. MXenes: New Horizons in Catalysis. *ACS Catal.* **2020**, *10*, 13487–13503. [CrossRef]
61. Xin, M.; Li, J.; Ma, Z.; Pan, L.; Shi, Y. MXenes and Their Applications in Wearable Sensors. *Front. Chem.* **2020**, *8*, 297. [CrossRef]
62. Li, N.; Peng, J.; Ong, W.-J.; Ma, T.; Arramel; Zhang, P.; Jiang, J.; Yuan, X.; Zhang, C. MXenes: An Emerging Platform for Wearable Electronics and Looking Beyond. *Matter* **2021**, *4*, 377–407. [CrossRef]
63. Huang, J.; Li, Z.; Mao, Y.; Li, Z. Progress and biomedical applications of MXenes. *Nano Select* **2021**, *2*, 1480–1508. [CrossRef]
64. Gogotsi, Y.; Huang, Q. MXenes: Two-Dimensional Building Blocks for Future Materials and Devices. *ACS Nano* **2021**, *15*, 5775–5780. [CrossRef] [PubMed]
65. Liang, R.; Li, Y.; Huo, M.; Lin, H.; Chen, Y. Triggering Sequential Catalytic Fenton Reaction on 2D MXenes for Hyperthermia-Augmented Synergistic Nanocatalytic Cancer Therapy. *ACS Appl. Mater. Interfaces* **2019**, *11*, 42917–42931. [CrossRef]
66. Szuplewska, A.; Kulpińska, D.; Dybko, A.; Chudy, M.; Jastrzębska, A.M.; Olszyna, A.; Brzózka, Z. Future Applications of MXenes in Biotechnology, Nanomedicine, and Sensors. *Trends Biotechnol.* **2020**, *38*, 264–279. [CrossRef] [PubMed]
67. Cui, Y.; Zhang, D.; Shen, K.; Nie, S.; Liu, M.; Huang, H.; Deng, F.; Zhou, N.; Zhang, X.; Wei, Y. Biomimetic anchoring of Fe_3O_4 onto Ti_3C_2 MXene for highly efficient removal of organic dyes by Fenton reaction. *J. Environ. Chem. Eng.* **2020**, *8*, 104369. [CrossRef]
68. Ma, Y.; Lv, X.; Xiong, D.; Zhao, X.; Zhang, Z. Catalytic degradation of ranitidine using novel magnetic Ti_3C_2-based MXene nanosheets modified with nanoscale zero-valent iron particles. *Appl. Catal. B Environ.* **2020**, *284*, 119720. [CrossRef]
69. Wojciechowska, A. Colloidal Properties and Stability of 2D Ti3C2 and Ti2C MXenes in Water. *Int. J. Electrochem. Sci.* **2018**, *13*, 10837–10847.
70. Orimolade, B.O.; Idris, A.O.; Feleni, U.; Mamba, B. Recent advances in degradation of pharmaceuticals using Bi_2WO_6 mediated photocatalysis—A comprehensive review. *Environ. Pollut.* **2021**, *289*, 117891. [CrossRef]
71. Jiang, X.; Kuklin, A.V.; Baev, A.; Ge, Y.; Ågren, H.; Zhang, H.; Prasad, P.N. Two-dimensional MXenes: From morphological to optical, electric, and magnetic properties and applications. *Phys. Rep.* **2020**, *848*, 1–58. [CrossRef]
72. Cheng, X.; Zu, L.; Jiang, Y.; Shi, D.; Cai, X.; Ni, Y.; Lin, S.; Qin, Y. A titanium-based photo-Fenton bifunctional catalyst of mp-MXene/TiO_{2-x} nanodots for dramatic enhancement of catalytic efficiency in advanced oxidation processes. *Chem. Comm.* **2018**, *54*, 11622–11625. [CrossRef]
73. Zhang, L.; Wang, H.; Chen, Z.; Wong, P.K.; Liu, J. Bi_2WO_6 micro/nanostructures: Synthesis, modifications and visible-light-driven photocatalytic applications. *Appl. Catal. B Environ.* **2011**, *106*, 1–13.
74. Kong, X.Y.; Lee, W.Q.; Mohamed, A.R.; Chai, S.-P. Effective steering of charge flow through synergistic inducing oxygen vacancy defects and p-n heterojunctions in 2D/2D surface-engineered Bi_2WO_6/BiOI cascade: Towards superior photocatalytic CO_2 reduction activity. *Chem. Eng. J.* **2019**, *372*, 1183–1193. [CrossRef]
75. Huang, T.; Li, Y.; Wu, X.; Lv, K.; Li, Q.; Li, M.; Du, D.; Ye, H. In-situ transformation of Bi_2WO_6 to highly photoreactive Bi_2WO_6@Bi_2S_3 nanoplate via ion exchange. *Chin. J. Catal.* **2018**, *39*, 718–727. [CrossRef]
76. Qin, Y.; Li, H.; Lu, J.; Ding, Y.; Ma, C.; Liu, X.; Meng, M.; Yan, Y. Fabrication of Bi_2WO_6/In_2O_3 photocatalysts with efficient photocatalytic performance for the degradation of organic pollutants: Insight into the role of oxygen vacancy and heterojunction. *Adv. Powder Technol.* **2020**, *31*, 2890–2900. [CrossRef]
77. Yang, R.; Zhong, S.; Zhang, L.; Liu, B. PW12/CN@Bi_2WO_6 composite photocatalyst prepared based on organic-inorganic hybrid system for removing pollutants in water. *Sep. Purif. Technol.* **2020**, *235*, 116270. [CrossRef]
78. Zhang, C.; Chen, G.; Lv, C.; Yao, Y.; Xu, Y.; Jin, X.; Meng, Q. Enabling Nitrogen Fixation on Bi_2WO_6 Photocatalyst by c-PAN Surface Decoration. *ACS Sustain. Chem. Eng.* **2018**, *6*, 11190–11195. [CrossRef]

79. Guo, L.; Zhang, K.; Han, X.; Zhao, Q.; Zhang, Y.; Qi, M.; Wang, D.; Fu, F. 2D/2D type-II Cu_2ZnSnS_4/Bi_2WO_6 heterojunctions to promote visible-light-driven photo-Fenton catalytic activity. *Chin. J. Catal.* **2020**, *41*, 503–513. [CrossRef]
80. Jiang, J.; Gao, J.; Niu, S.; Wang, X.; Li, T.; Liu, S.; Lin, Y.; Xie, T.; Dong, S. Comparing dark- and photo-Fenton-like degradation of emerging pollutant over photo-switchable $Bi(_2)WO(_6)/CuFe(_2)O(_4)$: Investigation on dominant reactive oxidation species. *J. Environ. Sci.* **2021**, *106*, 147–160. [CrossRef]
81. Zhong, X.; Wu, W.-T.; Jie, H.-N.; Tang, W.-Y.; Chen, D.-Y.; Ruan, T.; Bai, H.-P. Degradation of norfloxacin by copper-doped Bi_2WO_6-induced sulfate radical-based visible light-Fenton reaction. *RSC Adv.* **2020**, *10*, 38024–38032. [CrossRef]
82. Pamei, M.; Puzari, A. Luminescent transition metal-organic frameworks: An emerging sensor for detecting biologically essential metal ions. *Nano-Struct. Nano-Objects* **2019**, *19*, 100364. [CrossRef]
83. O'Keeffe, M.; Yaghi, O.M. Deconstructing the crystal structures of metal-organic frameworks and related materials into their underlying nets. *Chem. Rev.* **2012**, *112*, 675–702. [CrossRef] [PubMed]
84. Howarth, A.J.; Liu, Y.; Li, P.; Li, Z.; Wang, T.C.; Hupp, J.T.; Farha, O.K. Chemical, thermal and mechanical stabilities of metal-organic frameworks. *Nat. Rev. Mater.* **2016**, *1*, 15018. [CrossRef]
85. Zhao, M.; Huang, Y.; Peng, Y.; Huang, Z.; Ma, Q.; Zhang, H. Two-dimensional metal-organic framework nanosheets: Synthesis and applications. *Chem. Soc. Rev.* **2018**, *47*, 6267–6295. [CrossRef] [PubMed]
86. Jiao, L.; Seow, J.Y.R.; Skinner, W.S.; Wang, Z.U.; Jiang, H.-L. Metal-organic frameworks: Structures and functional applications. *Mater. Today* **2019**, *27*, 43–68. [CrossRef]
87. Huang, C.-W.; Nguyen, V.-H.; Zhou, S.-R.; Hsu, S.-Y.; Tan, J.-X.; Wu, K.C.W. Metal-organic frameworks: Preparation and applications in highly efficient heterogeneous photocatalysis. *Sustain. Energy Fuels* **2020**, *4*, 504–521. [CrossRef]
88. Wu, Q.; Yang, H.; Kang, L.; Gao, Z.; Ren, F. Fe-based metal-organic frameworks as Fenton-like catalysts for highly efficient degradation of tetracycline hydrochloride over a wide pH range: Acceleration of Fe(II)/Fe(III) cycle under visible light irradiation. *Appl. Catal. B Environ.* **2020**, *263*, 118282. [CrossRef]
89. Bai, W.; Li, S.; Ma, J.; Cao, W.; Zheng, J. Ultrathin 2D metal-organic framework (nanosheets and nanofilms)-based xD–2D hybrid nanostructures as biomimetic enzymes and supercapacitors. *J. Mater. Chem. A* **2019**, *7*, 9086–9098. [CrossRef]
90. Mu, J.; Liu, J.; Ran, Z.; Arif, M.; Gao, M.; Wang, C.; Ji, S. Critical Role of CUS in the Au/MOF-808(Zr) Catalyst for Reaction of CO_2 with Amine/H_2 via *N*-Methylation and *N*-Formylation. *Ind. Eng. Chem. Res.* **2020**, *59*, 6543–6555. [CrossRef]
91. Ma, D.; Li, B.; Liu, K.; Zhang, X.; Zou, W.; Yang, Y.; Li, G.; Shi, Z.; Feng, S. Bifunctional MOF heterogeneous catalysts based on the synergy of dual functional sites for efficient conversion of CO_2 under mild and co-catalyst free conditions. *J. Mater. Chem. A* **2015**, *3*, 23136–23142. [CrossRef]
92. Yoo, D.K.; Bhadra, B.N.; Jhung, S.H. Adsorptive removal of hazardous organics from water and fuel with functionalized metal-organic frameworks: Contribution of functional groups. *J. Hazard. Mater.* **2021**, *403*, 123655. [CrossRef]
93. Liu, H.; Yin, H.; Zhu, M.; Dang, Z. Degradation of organophosphorus flame retardants in heterogeneous photo-Fenton system driven by Fe(III)-based metal organic framework: Intermediates and their potential interference on bacterial metabolism. *Chemosphere* **2021**, *291*, 133072. [CrossRef] [PubMed]
94. Ghasempour, H.; Wang, K.-Y.; Powell, J.A.; ZareKarizi, F.; Lv, X.-L.; Morsali, A.; Zhou, H.-C. Metal-organic frameworks based on multicarboxylate linkers. *Coord. Chem. Rev.* **2021**, *426*, 213542. [CrossRef]
95. Mu, W.; Liu, D.; Yang, Q.; Zhong, C. Computational study of the effect of organic linkers on natural gas upgrading in metal-organic frameworks. *Microporous Mesoporous Mater.* **2010**, *130*, 76–82. [CrossRef]
96. Virender, K.S. Water depollution using metal-organic frameworks-catalyzed advanced oxidation processes: A review. *J. Hazard. Mater.* **2019**, *372*, 3–16.
97. Laurier, K.G.M.; Fron, E.; Atienzar, P.; Kennes, K.; Garcia, H.; Van der Auweraer, M.; De Vos, D.E.; Hofkens, J.; Roeffaers, M.B.J. Delayed electron-hole pair recombination in iron(iii)-oxo metal-organic frameworks. *Phys. Chem. Chem. Phys.* **2014**, *16*, 5044–5047. [CrossRef]
98. Zheng, F.; Xiang, D.; Li, P.; Zhang, Z.; Du, C.; Zhuang, Z.; Li, X.; Chen, W. Highly Conductive Bimetallic Ni-Fe Metal Organic Framework as a Novel Electrocatalyst for Water Oxidation. *ACS Sustain. Chem. Eng.* **2019**, *7*, 9743–9749. [CrossRef]
99. Wang, X.; Zhou, W.; Wu, Y.-P.; Tian, J.-W.; Wang, X.-K.; Huang, D.-D.; Zhao, J.; Li, D.-S. Two facile routes to an AB & Cu-MOF composite with improved hydrogen evolution reaction. *J. Alloys Compd.* **2018**, *753*, 228–233.
100. Soetaredjo, F.E.; Santoso, S.P.; Lunardi, V.B.; Kurniawan, A.; Shuwanto, H.; Lie, J.; Foe, K.; Irawaty, W.; Yuliana, M.; Putro, J.N.; et al. Highly efficient degradation of organic pollutant mixtures by a Fe(III)-based MOF-catalyzed Fenton-like process in subcritical water. *J. Mol. Liq.* **2021**, *347*, 117989. [CrossRef]
101. Ye, Z.; Schukraft, G.E.M.; L'Hermitte, A.; Xiong, Y.; Brillas, E.; Petit, C.; Sirés, I. Mechanism and stability of an Fe-based 2D MOF during the photoelectro-Fenton treatment of organic micropollutants under UVA and visible light irradiation. *Water Res.* **2020**, *184*, 115986. [CrossRef]
102. Wang, F.-X.; Wang, C.-C.; Du, X.; Li, Y.; Wang, F.; Wang, P. Efficient removal of emerging organic contaminants via photo-Fenton process over micron-sized Fe-MOF sheet. *Chem. Eng. J.* **2022**, *429*, 132495. [CrossRef]
103. Ameta, R.; Chohadia, A.K.; Jain, A.; Punjabi, P.B. Chapter 3—Fenton and Photo-Fenton Processes. In *Advanced Oxidation Processes for Waste Water Treatment*; Ameta, S.C., Ameta, R., Eds.; Academic Press: Cambridge, MA, USA, 2018; pp. 49–87.
104. Liao, C.-H.; Gurol, M.D. Chemical Oxidation by Photolytic Decomposition of Hydrogen Peroxide. *Environ. Sci. Technol.* **1995**, *29*, 3007–3014. [CrossRef] [PubMed]

105. Liao, C.-H.; Kang, S.-F.; Wu, F.-A. Hydroxyl radical scavenging role of chloride and bicarbonate ions in the H_2O_2/UV process. *Chemosphere* **2001**, *44*, 1193–1200. [CrossRef]
106. Wu, Y.; Li, X.; Zhao, H.; Yao, F.; Cao, J.; Chen, Z.; Ma, F.; Wang, D.; Yang, Q. 2D/2D FeNi-layered double hydroxide/bimetal-MOFs nanosheets for enhanced photo-Fenton degradation of antibiotics: Performance and synergetic degradation mechanism. *Chemosphere* **2021**, *287 Pt 1*, 132061. [CrossRef] [PubMed]
107. Tao, X.; Yuan, X.; Huang, L.; Shang, S.; Xu, D. Fe-based metal-organic frameworks as heterogeneous catalysts for highly efficient degradation of wastewater in plasma/Fenton-like systems. *RSC Adv.* **2020**, *10*, 36363–36370. [CrossRef]
108. Barreiro, J.C.; Capelato, M.D.; Martin-Neto, L.; Bruun Hansen, H.C. Oxidative decomposition of atrazine by a Fenton-like reaction in a H_2O_2/ferrihydrite system. *Water Res.* **2007**, *41*, 55–62. [CrossRef] [PubMed]
109. Pliego, G.; Zazo, J.A.; Garcia-Muñoz, P.; Munoz, M.; Casas, J.A.; Rodriguez, J.J. Trends in the Intensification of the Fenton Process for Wastewater Treatment: An Overview. *Crit. Rev. Environ. Sci. Technol.* **2015**, *45*, 2611–2692. [CrossRef]
110. Jiang, C.-C.; Zhang, J.-F. Progress and prospect in electro-Fenton process for wastewater treatment. *J. Zhejiang Univ. Sci. A* **2007**, *8*, 1118–1125. [CrossRef]
111. Pala, A.; Erden, G. Decolorization of a baker's yeast industry effluent by Fenton oxidation. *J. Hazard. Mater.* **2005**, *127*, 141–148. [CrossRef]
112. Seo, D.C.; Lee, H.J.; Hwang, H.N.; Park, M.R.; Kwak, N.W.; Cho, I.J.; Cho, J.S.; Seo, J.Y.; Joo, W.H.; Park, K.H.; et al. Treatment of non-biodegradable cutting oil wastewater by ultrasonication-Fenton oxidation process. *Water Sci. Technol.* **2007**, *55*, 251–259. [CrossRef]
113. Kumar, A.; Rana, A.; Sharma, G.; Naushad, M.; Dhiman, P.; Kumari, A.; Stadler, F.J. Recent advances in nano-Fenton catalytic degradation of emerging pharmaceutical contaminants. *J. Mol. Liq.* **2019**, *290*, 111177. [CrossRef]
114. Ihsanullah, I. MXenes (two-dimensional metal carbides) as emerging nanomaterials for water purification: Progress, challenges and prospects. *Chem. Eng. J.* **2020**, *388*, 124340. [CrossRef]
115. Du, X.; Fu, W.; Su, P.; Cai, J.; Zhou, M. Internal-micro-electrolysis-enhanced heterogeneous electro-Fenton process catalyzed by Fe/Fe3C@PC core-shell hybrid for sulfamethazine degradation. *Chem. Eng. J.* **2020**, *398*, 125681. [CrossRef]
116. Casado, J. Towards industrial implementation of Electro-Fenton and derived technologies for wastewater treatment: A review. *J. Environ. Chem. Eng.* **2019**, *7*, 102823. [CrossRef]
117. Luo, S.; Wang, R.; Yin, J.; Jiao, T.; Chen, K.; Zou, G.; Peng, Q. Preparation and Dye Degradation Performances of Self-Assembled MXene-Co_3O_4 Nanocomposites Synthesized via Solvothermal Approach. *ACS Omega* **2019**, *4*, 3946–3953. [CrossRef]
118. Rosales, E.; Pazos, M.; Sanromán, M.A. Advances in the Electro-Fenton Process for Remediation of Recalcitrant Organic Compounds. Chem. *Eng. Technol.* **2012**, *35*, 609–617. [CrossRef]
119. Muñoz-Écija, T.; Vargas-Quesada, B.; Chinchilla-Rodríguez, Z. Identification and visualization of the intellectual structure and the main research lines in nanoscience and nanotechnology at the worldwide level. *J. Nanopart. Res.* **2017**, *19*, 62. [CrossRef] [PubMed]
120. Ray, P.C.; Yu, H.; Fu, P.P. Toxicity and environmental risks of nanomaterials: Challenges and future needs. *J. Environ. Sci. Health C* **2009**, *27*, 1–35. [CrossRef]
121. Gupta, A.; Kumar, S.; Kumar, V. Challenges for Assessing Toxicity of Nanomaterials. In *Biochemical Toxicology—Heavy Metals and Nanomaterials*; IntechOpen: London, UK, 2019.
122. Arvidsson, R.; Molander, S.; Sandén, B.A.; Hassellöv, M. Challenges in Exposure Modeling of Nanoparticles in Aquatic Environments. Hum. Ecol. *Risk Assess.* **2011**, *17*, 245–262. [CrossRef]
123. Jahnel, J. Chapter 3.2—Addressing the Challenges to the Risk Assessment of Nanomaterials. In *Nanoengineering*; Dolez, P.I., Ed.; Elsevier: Amsterdam, The Netherlands, 2015; pp. 485–521.
124. Sun, W.; Wu, F.-G. Two-Dimensional Materials for Antimicrobial Applications: Graphene Materials and Beyond. *Chem. Asian J.* **2018**, *13*, 3378–3410. [CrossRef]
125. Linklater, D.P.; Baulin, V.A.; Juodkazis, S.; Ivanova, E.P. Mechano-bactericidal mechanism of graphene nanomaterials. *Interface Focus* **2018**, *8*, 20170060. [CrossRef]
126. Lu, X.; Feng, X.; Werber, J.R.; Chu, C.; Zucker, I.; Kim, J.H.; Osuji, C.O.; Elimelech, M. Enhanced antibacterial activity through the controlled alignment of graphene oxide nanosheets. *Proc. Natl. Acad. Sci. USA* **2017**, *114*, E9793–E9801. [CrossRef] [PubMed]
127. Chen, J.; Peng, H.; Wang, X.; Shao, F.; Yuan, Z.; Han, H. Graphene oxide exhibits broad-spectrum antimicrobial activity against bacterial phytopathogens and fungal conidia by intertwining and membrane perturbation. *Nanoscale* **2014**, *6*, 1879–1889. [CrossRef] [PubMed]
128. Akhavan, O.; Ghaderi, E. Toxicity of Graphene and Graphene Oxide Nanowalls Against Bacteria. *ACS Nano* **2010**, *4*, 5731–5736. [CrossRef] [PubMed]
129. Hu, J.; Wang, D.; Wang, J.; Wang, J. Bioaccumulation of Fe_2O_3(magnetic) nanoparticles in Ceriodaphnia dubia. *Environ. Pollut.* **2012**, *162*, 216–222. [CrossRef]
130. Krishnamoorthy, K.; Umasuthan, N.; Mohan, R.; Lee, J.; Kim, S.-J. Antibacterial Activity of Graphene Oxide Nanosheets. *Sci. Adv. Mater.* **2012**, *4*, 1–7. [CrossRef]
131. Gurunathan, S.; Han, J.W.; Dayem, A.A.; Eppakayala, V.; Kim, J.H. Oxidative stress-mediated antibacterial activity of graphene oxide and reduced graphene oxide in Pseudomonas aeruginosa. *Int. J. Nanomed.* **2012**, *7*, 5901–5914. [CrossRef]
132. Gurunathan, S.; Han, J.W.; Dayem, A.A.; Eppakayala, V.; Park, M.R.; Kwon, D.N.; Kim, J.H. Antibacterial activity of dithiothreitol reduced graphene oxide. *J. Ind. Eng. Chem.* **2013**, *19*, 1280–1288. [CrossRef]
133. Chen, J.; Wang, X.; Han, H. A new function of graphene oxide emerges: Inactivating phytopathogenic bacterium Xanthomonas oryzae pv. *Oryzae. J. Nanopart. Res.* **2013**, *15*, 1658. [CrossRef]

134. Karwowska, E. Antibacterial potential of nanocomposite-based materials—A short review. *Nanotechnol. Rev.* **2017**, *6*, 243–254. [CrossRef]
135. Jakubczak, M.; Jastrzębska, A.M. A Review on Development of Ceramic-Graphene Based Nanohybrid Composite Systems in Biological Applications. *Front. Chem.* **2021**, *9*, 685014. [CrossRef]
136. Wang, L.; Hu, C.; Shao, L. The antimicrobial activity of nanoparticles: Present situation and prospects for the future. *Int. J. Nanomed.* **2017**, *12*, 1227–1249. [CrossRef] [PubMed]
137. Chojnacka, K.; Mikulewicz, M. Bioaccumulation. In *Encyclopedia of Toxicology*, 3rd ed.; Wexler, P., Ed.; Academic Press: Oxford, UK, 2014; pp. 456–460.
138. Jain, B.; Singh, A.K.; Kim, H.; Lichtfouse, E.; Sharma, V.K. Treatment of organic pollutants by homogeneous and heterogeneous Fenton reaction processes. *Environ. Chem. Lett.* **2018**, *16*, 947–967. [CrossRef]
139. Saratale, R.G.; Sivapathan, S.; Saratale, G.D.; Banu, J.R.; Kim, D.S. Hydroxamic acid mediated heterogeneous Fenton-like catalysts for the efficient removal of Acid Red 88, textile wastewater and their phytotoxicity studies. *Ecotoxicol. Environ. Saf.* **2019**, *167*, 385–395. [CrossRef] [PubMed]
140. Kwarciak-Kozłowska, A. Chapter 7—Removal of pharmaceuticals and personal care products by ozonation, advance oxidation processes, and membrane separation. In *Pharmaceuticals and Personal Care Products: Waste Management and Treatment Technology*; Prasad, M.N.V., Vithanage, M., Kapley, A., Eds.; Butterworth-Heinemann: Oxford, UK, 2019; pp. 151–171.
141. Wu, Y.; Song, X.; Xu, W.; Sun, K.-Y.; Wang, Z.; Lv, Z.; Wang, Y.; Wang, Y.; Zhong, W.; Wei, J.; et al. NIR-Activated Multimodal Photothermal/Chemodynamic/Magnetic Resonance Imaging Nanoplatform for Anticancer Therapy by Fe(II) Ions Doped MXenes (Fe-Ti_3C_2). *Small* **2021**, *17*, 2101705. [CrossRef] [PubMed]
142. Meister, A. Biosynthesis and functions of glutathione, an essential biofactor. *J. Nutr. Sci. Vitaminol.* **1992**, *38*, 1–6. [CrossRef]